Course Outline

1. Symmetry, Group Theory, and Electronic Structure

1.1 Fundamentals

1.2 Symmetry and Group Theory

1.3 Vibrational Spectroscopy

2. Ground State Spectroscopic Methods

3. Excited State Spectroscopic Methods

4. Other Physical Methods

Basic Concepts – Vibrational Spectroscopy

- molecules are not static entities
  - they move around → translations
  - they turn on themselves → rotations
  - they change shape → vibrations
  - occur @ very different energies (decoupled?)
- molecular vibrations are extremely important for chemical processes
  - major mechanism for molecular transformations:
    - vibrational mode ↔ reaction coordinate
  - normally think of changes in nuclear positions
    - electronic structure is affected as well
    - change of electron cloud = change in behavior
    - vibrational forces = chemical bonding!
- vibrational spectroscopy can therefore be extremely useful!

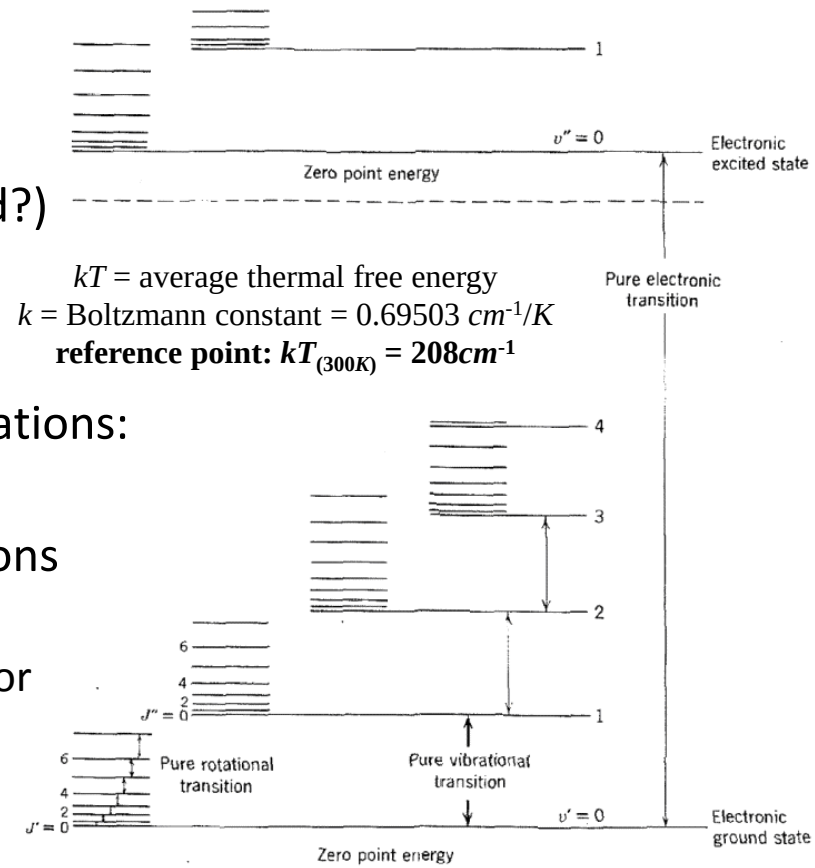

kT = average thermal free energy
k = Boltzmann constant = 0.69503 cm^{-1}/K
reference point: $kT_{(300K)} = 208cm^{-1}$

Potential Energy Curves & Surfaces

- potential energy surfaces (PES) provide classical representation of energetics
  - energy changes along all possible degrees of freedom (3N dimensional space!)
  - usually show PES only along chemically "useful" coordinates
    - specific normal modes of vibration
    - reaction coordinate (geometric changes that get you from reactants to products)
- simplest example – homonuclear diatomic molecule
  - one chemically relevant coordinate $\rightarrow$ bond distance (Δr) $\rightarrow$ potential energy curve
  - combination of several important energetic contributions
    - macroscopic electrostatic attraction/repulsion (ionic bonding)
    - overlap of atomic orbitals for electron sharing (covalent bonding)
- simplest approximation of chemical bond $\rightarrow$ harmonic oscillator
  - follows Hooke's Law
  - symmetrical potential
  - assumes one finite mass connected to infinite mass

$$F = ma = -kx \quad \Rightarrow \quad \boxed{\nu = \frac{1}{2\pi}\sqrt{\frac{k}{m}}}$$

1.3 Vibrational Spectroscopy

- harmonic oscillator follows Hooke's Law

$$F = ma = -kx \quad \Rightarrow \quad \boxed{\nu = \frac{1}{2\pi}\sqrt{\frac{k}{m}}}$$

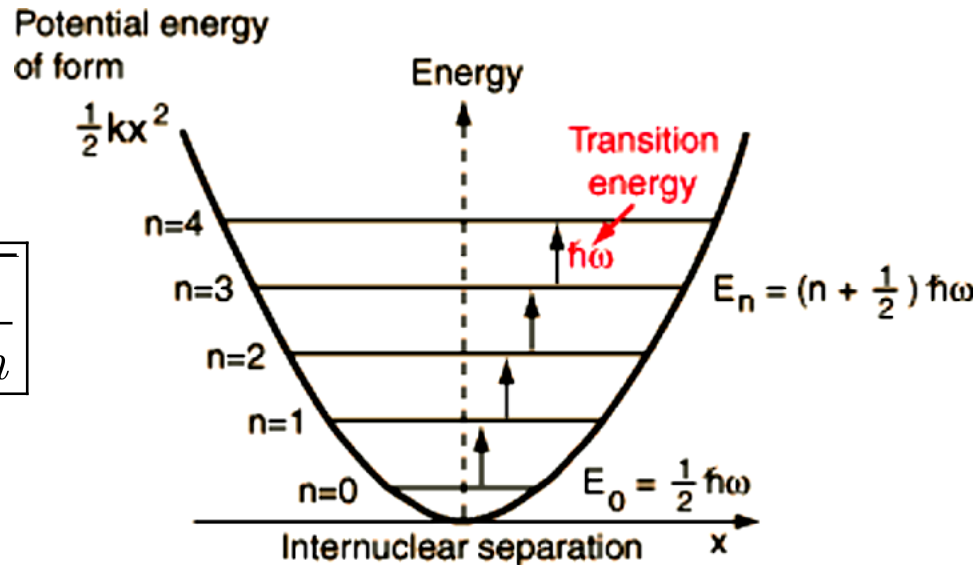

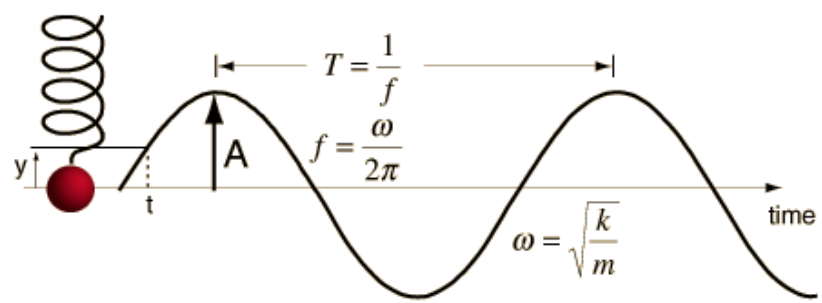

1.3 Vibrational Spectroscopy

- simple harmonic oscillator reasonable near equilibrium → small Δr
- must be 'fixed' to account for the fact that each atom has a mass
  - use 'reduced mass' (μ) of system instead of m
  - describes complete system as having a single μ about which everything happens

$$\mu = \frac{m_1 m_2}{m_1 + m_2}$$

- SHO model cannot account for anharmonicity in bond vibrations
  - bond dissociation at large Δr
  - huge internuclear repulsion at short Δr
  - need better approximation
- use Morse potential function $\boxed{E = D\ 1 - e^{-\beta x}\ ^2}$
  - reasonable bond potential energies
  - enforces anharmonic behavior
  - in cm^{-1}:

$$\boxed{\tilde{\upsilon}_{v \to v+1} = \tilde{\upsilon}_{SHO} - \frac{v+1\ \tilde{\upsilon}_{SHO}^2}{2D}}$$

$$\text{where } \tilde{\upsilon}_{SHO} = \frac{1}{2\pi c}\sqrt{\frac{k}{\mu}}$$

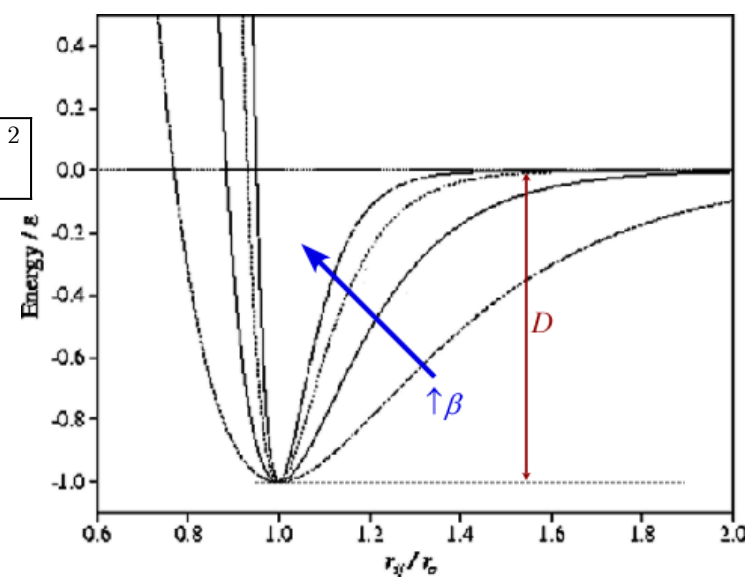

Basic Concepts – Higher Dimensional Surfaces

- every vibrational degree of freedom has an energy profile
  - stretching/contraction modes will have profiles that are similar to Morse potential
  - bond angles and dihedrals will have more periodic behavior (no dissociation)
- complete potential energy description involves all degrees of freedom
  - generally extremely complex → 3*N*-6 vibrational degrees of freedom
  - can visually represent only two degrees of freedom at a time to give a surface plot...
- Boltzmann energies available at RT are very small (~200 cm^{-1})
  - only lowest vib levels are populated
  - vibrational spectroscopy probes bottom of potential energy well
- Vibrational spectroscopy is exp probe of potential energy surfaces

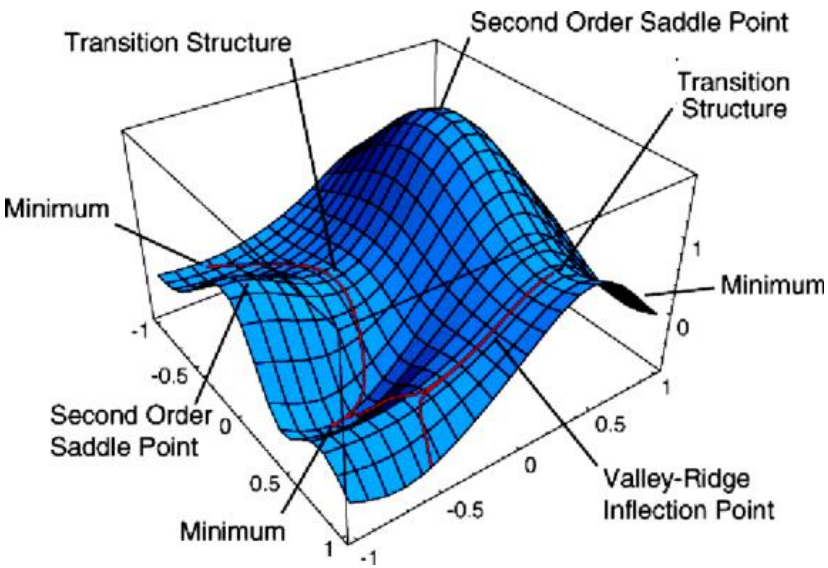

Approaches to Vibrational Spectroscopy

- infrared absorption spectroscopy (IR)
  - direct photon absorption (50-5000 cm^{-1})
  - requires *change in electric dipole moment*
  - basic selection rule: $\Delta v = \pm 1$

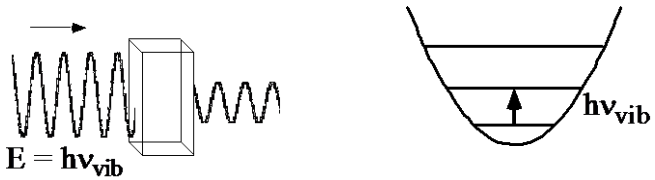

- Raman spectroscopy
  - indirect photon scattering (usually UV/Vis/NIR)
  - requires *change in polarizability* of molecule
  - basic selection rule: $\Delta v = \pm 1$

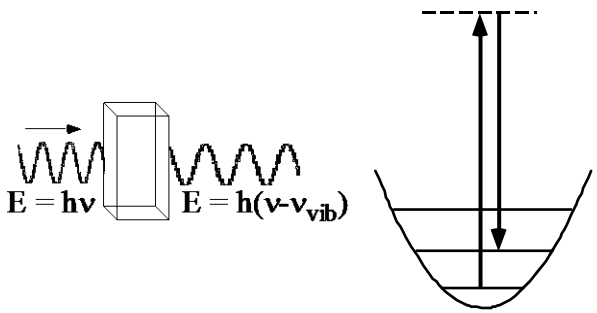

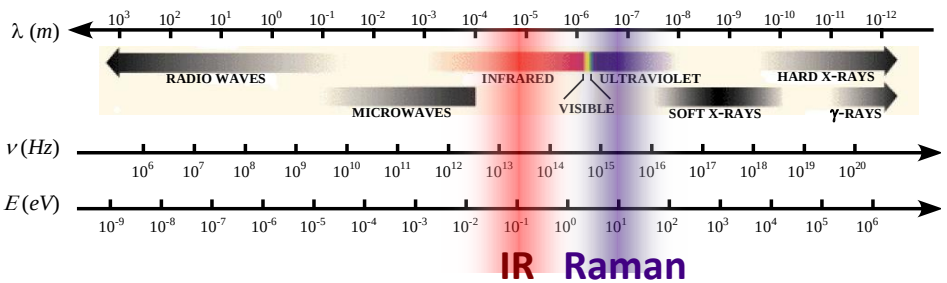

Symmetry of molecular vibrational modes

- use SHO to describe vibrational modes of molecules
- characteristics of infrared absorption:
  - transition energies: $E_{0\to1}(eV) = \frac{\hbar}{2}\sqrt{\frac{k}{\mu}}$ $\quad \upsilon_{0\to1}(Hz) = \frac{1}{2\pi}\sqrt{\frac{k}{\mu}}$ $\quad \tilde{\upsilon}_{0\to1}(cm^{-1}) = \frac{1}{2\pi c}\sqrt{\frac{k}{\mu}}$
  - wavefunctions: $\psi_{v=n} = Ne^{-\frac{1}{2}(\upsilon/\hbar)q^2} H_n(\sqrt{\frac{\upsilon}{\hbar}}q) \rightarrow q$ is the vibrational coordinate and $H_n\ \sqrt{\frac{\upsilon}{\hbar}}q$ is a *Hermite polynomial*

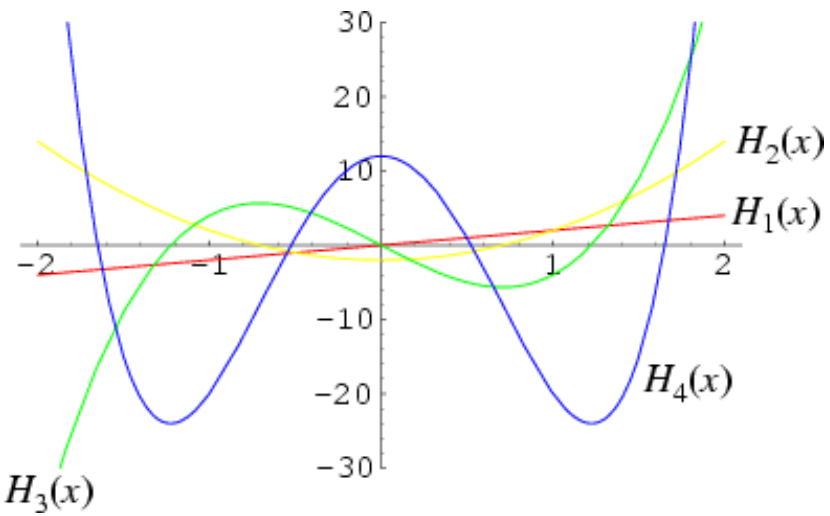

$H_0(x) = 1$	$\psi_0 = Ne^{-\frac{1}{2}(\upsilon/\hbar)q^2}$	*symmetric*
$H_1(x) = 2x$	$\psi_1 = Ne^{-\frac{1}{2}(\upsilon/\hbar)q^2}\ 2\sqrt{\frac{\upsilon}{\hbar}}q$	*antisymmetric*
$H_2(x) = 4x^2 - 2 \quad \Rightarrow$	$\psi_2 = Ne^{-\frac{1}{2}(\upsilon/\hbar)q^2}\ 4\ \frac{\upsilon}{\hbar}q^2\ +2$	
$H_3(x) = 8x^3 - 12x$	$\psi_3 = Ne^{-\frac{1}{2}(\upsilon/\hbar)q^2}\ 8\ \sqrt{\frac{\upsilon}{\hbar}}q\ ^3 - 12\sqrt{\frac{\upsilon}{\hbar}}q$	
…	…	

1.3 Vibrational Spectroscopy

- symmetry of odd wavefunctions depends on form of polynomial
  - focus on 0→1 transition because it is usually what is observed
  - *v* = 0 → always totally symmetric $\psi_0 = Ne^{-\frac{1}{2}(\upsilon/\hbar)q^2} = k\mathbf{G} \Rightarrow \text{a Gaussian function}$
  - *v* = 1 → depends on symmetry of *q* $\psi_1 = Ne^{-\frac{1}{2}(\upsilon/\hbar)q^2}\ 2\sqrt{\frac{\upsilon}{\hbar}}q\ = k\mathbf{G}q \Rightarrow \text{symmetry of } q$
- complete wavefunction includes product of vibrational states

$$\Psi_{q_1=0} \propto \psi_0^{q_1}\ \ \psi_0^{q_2}\ \ \psi_0^{q_3}\ \cdots \mapsto A_1\ \ A_1\ \ A_1\ \cdots \mapsto A_1$$

$$\Psi_{q_1=1} \propto \psi_1^{q_1}\ \ \psi_0^{q_2}\ \ \psi_0^{q_3}\ \cdots \mapsto \Gamma_{q_1}\ \ A_1\ \ A_1\ \cdots \mapsto \Gamma_{q_1}$$

- can simplify intensity equation for vibrational transitions
  - dominant term in transition moment operator → electric dipole operator
  - use symmetry to determine appropriate selection rules!

$$I_{0\to1}^{q_1} \propto \left|\left\langle \Psi_{\nu\ q_1=1} \middle| \hat{\mu} \middle| \Psi_{\nu\ q_1=0} \right\rangle\right|^2$$

$$\propto \left|\left\langle \psi^{q_1}_{\nu=1} \middle| \hat{\mu} \middle| \psi^{q_1}_{\nu=0} \right\rangle\right|^2$$

$$\hat{\mu} \sim \hat{\mu}_1 \rightarrow\ \vec{x}, \vec{y}, \vec{z}$$

1.3 Vibrational Spectroscopy

- *e.g.*, H_2O in C_{2v} symmetry
  - what vibrational transitions will be allowed? *i.e.*, what vibrations will be observed?

C_{2v}	E	C_2	σ_{xz}	σ_{yz}	
A_1	+1	+1	+1	+1	z, x^2, y^2, z^2
A_2	+1	+1	-1	-1	R_z, xy
B_1	+1	-1	+1	-1	x, R_y, xz
B_2	+1	-1	-1	+1	y, R_x, yz

$$I_{0\to1}^{q_1} \propto \left|\left\langle \psi_{v=1}^{q_1} \middle| \hat{\mu} \middle| \psi_{v=0}^{q_1} \right\rangle\right|^2$$
$$\to \Gamma_{v=1}^{q_1} \times \Gamma_{\mu_1} \times \Gamma_{v=0}^{q_1}$$
$$\to A_1 \times \Gamma_{x,y,z} \times \Gamma_{q_1}$$
$$\to \Gamma_{x,y,z} \times \Gamma_{q_1}$$

depends on symmetry of transition moment operator and the vibrational mode… they have to be the same!

symmetric stretch

$$S_{A_1} = \frac{1}{\sqrt{2}}(\Delta r_1 + \Delta r_2)$$

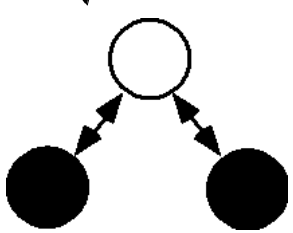

allowed along z-axis

asymmetric stretch

$$S_{B_1} = \frac{1}{\sqrt{2}}(\Delta r_1 - \Delta r_2)$$

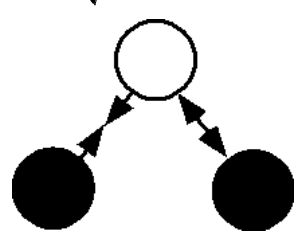

allowed along x-axis

bending

$$S_{A_1} = \Delta\theta$$

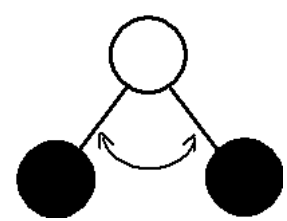

allowed along z-axis

1.3 Vibrational Spectroscopy

- *e.g.*, $[NO_3]^-$ in D_{3h} symmetry

$$\Gamma_{3N} = A_1' + A_2' + 3E' + 2A_2'' + E''$$

$$\Gamma_{vib} = \Gamma_{3N} - \Gamma_{trans} - \Gamma_{rot} = \Gamma_{3N} - \Gamma_{x,y,z} - \Gamma_{R_x,R_y,R_z}$$

$$= \Gamma_{3N} - \left[E' + A_2''\right] - \left[A_2' + E_2''\right]$$

$$= \boxed{A_1' + 2E' + A_2''}$$

D_{3h}	E	$2C_3$	$3C_2$	σ_h	$2S_3$	$3\sigma_v$	
A_1'	1	1	1	1	1	1	z^2
A_2'	1	1	-1	1	1	-1	R_z
E'	2	-1	0	2	-1	0	(x,y), (x^2-y^2,xy)
A_1''	1	1	1	-1	-1	-1	
A_2''	1	1	-1	-1	-1	1	z
E''	2	-1	0	-2	1	0	(R_x,R_y), (xz,yz)

$A_1' \mapsto \quad S_{A_1'}^{\Delta r} = \frac{1}{\sqrt{3}}\ \Delta r_1 + \Delta r_2 + \Delta r_3$

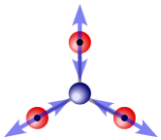

forbidden

$E' \mapsto \quad S_{E'}^{\Delta\vec{r}}(1) = \frac{1}{\sqrt{6}}\ 2\Delta\vec{r}_1 - \Delta\vec{r}_2 - \Delta\vec{r}_3$

$S_{E'}^{\Delta\vec{r}}(2) = \frac{1}{\sqrt{2}}\ \Delta\vec{r}_2 - \Delta\vec{r}_3$

allowed along (x,y)

$E' \mapsto \quad S_{E'}^{\Delta\vec{\theta}}(1) = \frac{1}{\sqrt{6}}\ 2\Delta\vec{\theta}_1 - \Delta\vec{\theta}_2 - \Delta\vec{\theta}_3$

$S_{E'}^{\Delta r}(2) = \frac{1}{\sqrt{2}}\ \Delta\vec{\theta}_2 - \Delta\vec{\theta}_3$

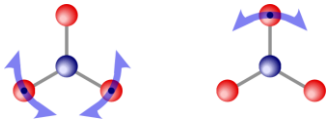

allowed along (x,y)

$A_2'' \mapsto \quad S_{A_2''}^{\Delta\vec{\phi}} = \frac{1}{\sqrt{3}}\ \Delta\vec{\phi}_1 + \Delta\vec{\phi}_2 + \Delta\vec{\phi}_3$

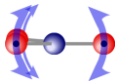

allowed along z

Normal Coordinate Analysis

- molecular vibrations known as the ***Normal Coordinates***
- these are linear combinations of internal coordinates (R_i), or symmetry coordinates (S_i)
- major characteristic of normal ("normalized") vibration
  - internal coords (R_1, R_2, ..., R_i) all oscillate at the same frequency
  - only their amplitudes of oscillation differ
- express relationship btw R_i (or S_i) & normal coordinates Q_i as

$$\begin{aligned} Q_1 &= l_{11}R_1 + l_{12}R_2 + \cdots + l_{1N}R_N \\ Q_2 &= l_{21}R_1 + l_{22}R_2 + \cdots + l_{2N}R_N \\ &\vdots \\ Q_N &= l_{N1}R_1 + l_{N2}R_2 + \cdots + l_{NN}R_N \end{aligned} \quad or \quad \mathbf{Q} = \mathbf{LR}$$

l_{ij} are the amplitude coefficients

Vibrational Force Constants

- SHO equation for potential energy: $V\ \ q\ = \frac{1}{2}kq^2$ where $k = \left(\frac{d^2V}{dq^2}\right)_{q\to 0}$
- solve QM-SHO problem, we find that $E_{SHO}(cm^{-1}) = \tilde{\upsilon}_{SHO}\ \ v + \frac{1}{2}$
  - the mass is the reduced mass: $\mu = \frac{m_1 m_2}{m_1 + m_2}$ $\tilde{\upsilon}_{SHO} = \frac{1}{2\pi c}\sqrt{\frac{k}{\mu}}$
  - example: HX

the reduced masses don't change very much, but the frequencies do!
must relate to force constants...

X	m_X	$\tilde{\upsilon}\ \ cm^{-1}$	μ
F	19.0	4138.5	0.95
Cl	35.5	2991	0.97
Br	79.9	2649.7	0.99
I	126.9	2309	0.99

  - vibrational frequencies relate to the nature of the bonding between atoms
- ***Badger's rule*** $\rightarrow$ correlation btw force constants & bond lengths

Badger's Rule (and modifications)

Inorg. Chem. **1987**, *26*, 2127-2132

Assignment of the Rhodium–Rhodium Stretching Frequency in $Rh_2(O_2CCH_3)_4L_2$ Complexes and the Crystal and Molecular Structure of $[C(NH_2)_3]_2[Rh(O_2CCH_3)_4Cl_2]$. Relationship between Vibrational Spectra and Structure

Vincent M. Miskowski,*† Richard F. Dallinger,‡ Gary G. Christoph,§ David E. Morris,§ George H. Spies,|| and William H. Woodruff*§

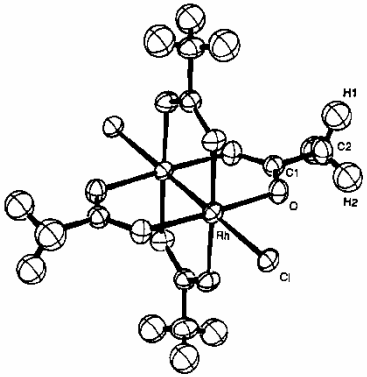

Figure 1. ORTEP drawing of the $[Rh_2(OAc)_4Cl_2]^{2-}$ structure in $[C(NH_2)_3]_2[Rh_2(OAc)_4Cl_2]$.

Figure 4. Plot of force constant vs. bond distance for bonds between elements of the row of the periodic table from Rb through I. The asterisk represents the point for a $Rh_2(OAc)_4$ unit having a Rh–Rh distance of 2.396 Å and ν(Rh–Rh) = 170 cm^{-1} (diatomic approximation for force constant). The open circle is the $Rh_2(OAc)_4$ point if the force constant is 2.60 mdyn/Å. The dashed lines are from ref 5. The solid line is the function from the present work, to be discussed in detail elsewhere.[6] Identity of points: (1) Cd metal; (2) Rh_2(2,5-diisocyano-2,5-dimethylhexane)$_4^{2+}$; (3) $Rh_2[CN(CH_2)_3NC]_4^{2+}$; (4) $[Rh(CNC_6H_5)_4]_2^{2+}$; (5) Sn metal; (6) RbI(g); (7) Zr metal; (8) Sn′ metal; (9) I_2(g) ($^3\Pi$); (10) $Tc_2(CO)_{10}$; (11) Cd′ metal; (12) I_3^-; (13) Te_2(g) (O_u^+); (14) $[Rh_2[CN(CH_2)_3NC]_4{\cdot}Cl_2]^{2+}$; (15) $Ru_3(CO)_{12}$; (16) CdTe(s); (17) Te_2(g) ($^3\Sigma_u^-$); (18) Sn(s, diamond); (19) InI(g) ($^1\Sigma^+$); (20) $[Rh_2$(2,5-diisocyano-2,5-dimethylhexane)$_4Cl_2]^{2+}$; (21) InI_3; (22) SbI_3; (23) Mo metal; (24) SnI_4; (25) I_2(g) ($^1\Sigma_g^+$); (26) $Mo_6Cl_{14}^{2-}$; (27) AgI(g) ($^1\Sigma^+$); (28) CdI_2; (29) Sb_2(g) (O_u^+); (30) Sb_2(g) ($^1\Sigma_g^+$); (31) $Ru(O_2CR)_4$; (32) $[Mo_2(HPO_4)_4{\cdot}2H_2O]^{2-}$; (33) $[Mo_2(HPO_4)_4{\cdot}Cl](Hpy)_3$; (34) $[Mo_2(CH_3)_8]^{4-}$; (35) $Mo_2I_4(PR_3)_4$; (36) $[Mo_2Cl_8]^{4-}$; (37) $Mo_2Cl_4(PR_3)_4$, $Mo_2Br_4(PR_3)_4$; (38) $Mo_2(O_2CCF_3)_4{\cdot}2py$; (39) $[Mo_2(SO_4)_4]^{4-}$; (40) $[Mo_2(SO_4)_4]^{3-}$, $Ru_2(O_2CCH_3)_4Cl$; (41) $Mo_2Br_2(O_2C_6H_5)_2(PR_3)_2$; (42) $Mo_2[(CH_2)_2P(CH_3)_2]_4$; (43) $Mo_2(O_2CCF_3)_4$; (44) $Mo_2(O_2CR)_4$; (45) $Mo_2[C_6H_5C(NC_6H_5)_2]_4$; (46) Mo_2(2-methyl-6-oxopyridine)$_4$; (47) Mo_2(g) ($^1\Sigma_g^+$).

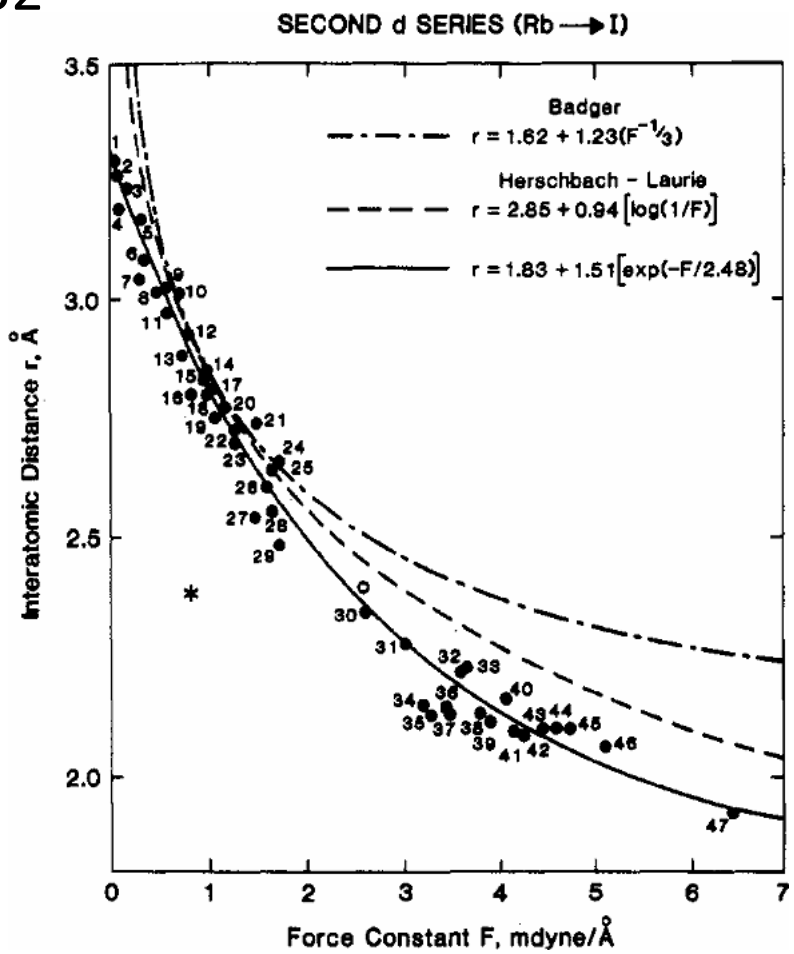

1.3 Vibrational Spectroscopy

Bond (XY)	Molecule	k_{XY}	Bond order
O-H	H_2O	8.4	1
C-C	CH_3CH_3	7.0	1
C=C	CH_2CH_2	14.2	2
C≡C	HCCH	24.5	3
C=C	C_6H_6	11.4	1.5
O=O	O_2	11.3	2
O-O	O_3	6.2	1.5
O-O	O_2^-	8.7	1.5
O-O	O_2^{2-}	6.2	1
N=O	NO^+	22.7	3
N=O	NO	15.5	2.5
N-O	NO^-	8.0	2

Typical force constants for small molecules...

- correlates with bond order for <u>related</u> molecules

The Wilson Method – a more quantitative approach

- rearrange energy expression: $\tilde{\nu} = \frac{1}{2\pi c}\sqrt{\frac{k}{\mu}} \quad \Rightarrow \quad \underbrace{4\pi^2 c^2 \tilde{\nu}^2}_{\lambda} = \frac{k}{\mu} \quad \Rightarrow \quad \boxed{\frac{k}{\mu} - \lambda = 0}$
  - three parameters of importance $\rightarrow$ ν, k, μ
  - given any two - the third can be easily determined
- above equation can be viewed as a [1$\times$1] secular determinant:
  - force matrix $\rightarrow$ $\mathbf{F}$
  - mass matrix $\rightarrow$ $\mathbf{G}$
  - energy matrix (in cm^{-1}) $\rightarrow$ $\mathbf{E}\lambda$
    - where **E** is the identity matrix (defines size of block matrix)
    - E matrix is (3*N*-6) $\times$ (3*N*-6) – over all vibrational modes...

$$|\mathbf{FG} - \mathbf{E}\lambda| = 0$$

- matrix approach can be used to solve vibrational modes...

1.3 Vibrational Spectroscopy

- *e.g.* H_2O modes $A_1^{(1)} \rightarrow 3657 cm^{-1}$ $A_1^{(2)} \rightarrow 1595 cm^{-1}$ $B_1 \rightarrow 3756 cm^{-1}$

$$V\ q_1, q_2, \ldots, q_N\ = \frac{1}{2}\sum_{m,n} k_{mn} q_m q_n$$

- we now have to deal with a multifrequency SHO such that $m \neq n$
- this means that we need to worry about interaction force constants (*i*) where
  - i.e. extent of coupling between modes of vibration (how does one affect the other)
- define vibrational modes in terms of internal coordinates:
- principal terms in the force constant matrix:
  - $k_{11} = k_{22}$ = restoring force for O-H stretch
  - k_{33} = restoring force for H-O-H bend
- Interaction force constants (off-diagonal terms):
  - $i_{12} = i_{21}$ (stretch-stretch interaction)
  - $i_{13} = i_{23} = i_{31} = i_{32}$ (stretch-bend interaction)

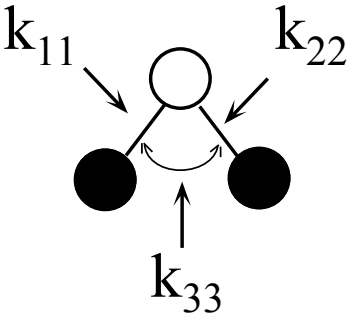

$$\mathbf{F} = \begin{bmatrix} k_{11} & i_{12} & i_{13} \\ i_{12} & k_{11} & i_{13} \\ i_{13} & i_{13} & k_{33} \end{bmatrix}$$

	Δr_1	Δr_2	$\Delta\theta$
Δr_1	k_{11}	i_{12}	i_{13}
Δr_2	i_{12}	k_{11}	i_{13}
$\Delta\theta$	i_{13}	i_{13}	k_{33}

1.3 Vibrational Spectroscopy

- choosing appropriate interaction terms (they are not observables)
  - **Simple Valence Approach**
    - simplest but least accurate
    - no off-diagonal force constants
  - **General Valence Force Field (GVFF)**
    - more intuitive, but harder to implement - used for simpler systems
    - off-diagonal terms treated as interaction terms (what we just did)
  - **Urey-Bradley Force Field**
    - easier to implement, at the expense of insight - used for more complex systems
    - off-diagonal terms treated as weak repulsive interactions btw nonbonding atoms
  - such choices and appropriate interaction terms have been developed and implemented in computational programs that make estimates for you.
- the **G** matrix also needs to be evaluated in a similar manner
  - simply complex geometric problem
  - solutions for many simple cases have been derived and tabulated

$$\mathbf{G} = \begin{bmatrix} g_{11} & g_{12} & g_{13} \\ g_{12} & g_{11} & g_{13} \\ g_{13} & g_{13} & g_{33} \end{bmatrix}$$

1.3 Vibrational Spectroscopy

- for H_2O, the G-matrix is as follows:

$$\mathbf{G}_{H_2O} = \begin{bmatrix} \mu_3 + \mu_1 & \mu_3 \cos\theta & -\frac{\mu_3}{r}\sin\theta \\ \mu_3 \cos\theta & \mu_3 + \mu_1 & -\frac{\mu_3}{r}\sin\theta \\ -\frac{\mu_3}{r}\sin\theta & -\frac{\mu_3}{r}\sin\theta & \frac{2\mu_1}{r^2} + \frac{2\mu_3}{r^2}(1-\cos\theta) \end{bmatrix}$$

$$\mu_1 = \mu_H = \tfrac{1}{1.008} = 0.99206$$

$$\mu_3 = \mu_O = \tfrac{1}{15.995} = 0.06252$$

$$r = 0.96(\mathring{A})$$

$$\theta = 105^\circ$$

<u>just to confuse things</u>:
μ is not exactly the same
as previous reduced masses

- we can now use the **F** and **G** matrices to extract numerical values for the force constants:
  - we have the frequencies (a diagonal λ matrix)
  - we have the mass matrix
  - we can figure out the **F**-matrix!

- note that this requires us to solve cubic equations (3×3 matrix problem)
  - in general, the problem is even more complex → higher dimensionality
  - symmetry is the best way to simplify problem...

1.3 Vibrational Spectroscopy

- symmetrizing the matrices = modifying basis set to 'fit' the point group
  - this will turn the internal coordinates into symmetry coordinates ($R_i \rightarrow S_i$)
  - need a *transformation matrix* (**U**) that will perform transformation – the matrix form of the SALCs!

$$\begin{array}{c} \\ S_{A1}(1) \\ S_{A1}(2) \\ S_{B1} \end{array} \begin{array}{c} \begin{array}{ccc} \Delta r_1 & \Delta r_2 & \Delta\theta \end{array} \\ \begin{bmatrix} \frac{1}{\sqrt{2}} & \frac{1}{\sqrt{2}} & 0 \\ 0 & 0 & 1 \\ \frac{1}{\sqrt{2}} & -\frac{1}{\sqrt{2}} & 0 \end{bmatrix} \end{array}$$

must transform **F** and **G** matrices by doing

$$\mathbf{F_s} = \mathbf{U'FU}$$
$$\mathbf{G_s} = \mathbf{U'GU}$$

- symmetrize **F**

$$\mathbf{F_s} = \begin{bmatrix} \frac{1}{\sqrt{2}} & \frac{1}{\sqrt{2}} & 0 \\ 0 & 0 & 1 \\ \frac{1}{\sqrt{2}} & -\frac{1}{\sqrt{2}} & 0 \end{bmatrix} \begin{bmatrix} \mathrm{k}_{11} & \mathrm{i}_{12} & \mathrm{i}_{13} \\ \mathrm{i}_{12} & \mathrm{k}_{11} & \mathrm{i}_{13} \\ \mathrm{i}_{13} & \mathrm{i}_{13} & \mathrm{k}_{33} \end{bmatrix} \begin{bmatrix} \frac{1}{\sqrt{2}} & 0 & \frac{1}{\sqrt{2}} \\ \frac{1}{\sqrt{2}} & 0 & -\frac{1}{\sqrt{2}} \\ 0 & 1 & 0 \end{bmatrix} = \begin{bmatrix} \mathrm{k}_{11} + \mathrm{i}_{12} & \sqrt{2}\mathrm{i}_{13} & 0 \\ \sqrt{2}\mathrm{i}_{13} & \mathrm{k}_{33} & 0 \\ 0 & 0 & \mathrm{k}_{11} - \mathrm{i}_{12} \end{bmatrix}$$

1.3 Vibrational Spectroscopy

- symmetrize **G**

$$\mathbf{G_s} = \begin{bmatrix} \mu_1 + \mu_3(1+\cos\theta) & -\frac{\sqrt{2}\mu_3}{r}\sin\theta & 0 \\ -\frac{\sqrt{2}\mu_3}{r}\sin\theta & \frac{2}{r^2}(\mu_1 + \mu_3 - \mu_3\cos\theta) & 0 \\ 0 & 0 & \mu_1 + \mu_3(1-\cos\theta) \end{bmatrix}$$

- we can now simplify the problem to one 2×2 problem (A_1) and a 1×1 problem (B_1).
  - but still can't solve the problem with additional information – 3 vibrations with 4 unknowns
  - the interaction term is still our biggest problem!
  - this can be solved by **isotopic substitution**
    - assumption: changing mass of an atom but not its identity will not affect <u>force constants</u>

	H_2O	D_2O
$A_1^{(1)}$	3657 cm^{-1}	2671 cm^{-1}
$A_1^{(2)}$	1595 cm^{-1}	1178 cm^{-1}
B_1	3756 cm^{-1}	2788 cm^{-1}

$\xrightarrow{\textit{iterative process}}$

k_{11} = 8.428 *mdyne*/Å
k_{33} = 0.768 *mdyne*/Å
i_{12} = -0.105 *mdyne*/Å
i_{13} = 0.252 *mdyne*/Å

- last thing – figure out the eigenvectors (back to the original question!)

1.3 Vibrational Spectroscopy

- each eigenvector must satisfy $\mathbf{GF}l_N = l_N\lambda$ (*N* is specific eigenvector)
  - easily solved using matrix math - direct calculation of each l_N
  - for the A_1 vibrational modes in H_2O:

$$\begin{bmatrix} l_{11} & l_{12} \\ l_{21} & l_{22} \end{bmatrix} = \begin{bmatrix} 1.01683 & -0.06686 \\ 0.01274 & 1.52432 \end{bmatrix}$$

$$Q_{A_1(1)} = 1.01683 S_{A_1(1)} - 0.06686 S_{A_1(2)} \Rightarrow \nu_1 = 3657 cm^{-1}$$

$$Q_{A_1(2)} = 0.01274 S_{A_1(1)} + 1.52432 S_{A_1(2)} \Rightarrow \nu_2 = 1595 cm^{-1}$$

large mismatch between the stretch and bend energies

- often expressed as potential energy contributions (instead of distances)

$$V(Q_N) = \frac{1}{2} Q_N^2 \sum_{ij} F_{ij} l_{iN} l_{jN}$$

	λ_1	λ_2
$S_{A1}(1)$	8.60551	0.03721
$S_{A1}(2)$	0.00011	1.64459

or

	λ_1	λ_2
$S_{A1}(1)$	99.99%	2.21%
$S_{A1}(2)$	0.01%	97.79%

Energy Factoring – Simplifying the force field even further

- for most real systems, symmetry is not necessarily that helpful
  - molecular symmetry is very low or non-existent (everything mixes!)
  - use "effective symmetry" rather than real symmetry to simplify problem
  - use other ways of removing small contributions → energy factoring
- mixing decreases significant with energy separation
  - set interaction parameter to zero when ΔE is large
  - *e.g.*, for H_2O → set i_{13} to zero

$$\mathbf{F_S} = \begin{bmatrix} k_{11} + i_{12} & \cancel{\sqrt{2}i_{13}} & 0 \\ \cancel{\sqrt{2}i_{13}} & k_{33} & 0 \\ 0 & 0 & k_{11} - i_{12} \end{bmatrix}$$

← *note*: does not remove energy effect of i_{12}.

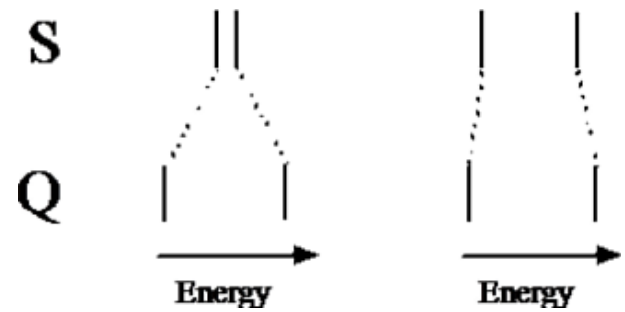

- concept of ***characteristic group frequencies***
  - consider certain atom 'groupings' together → their vibrational frequencies are coupled
  - generally corresponds with functionally-relevant groupings → this is no accident!

Higher order effects in IR spectroscopy

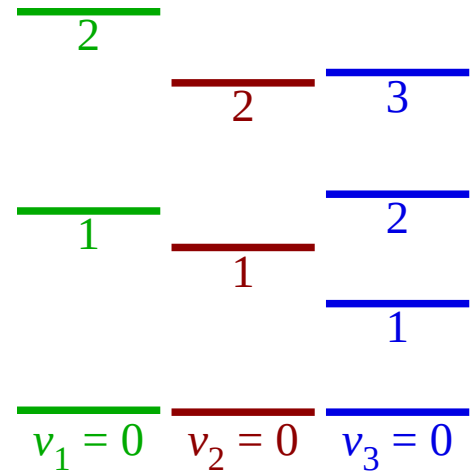

- anharmonicity in the potentials cause a breakdown in rigorous selection rules $\rightarrow \Delta v = 1$
  - can allow higher-order transitions to be visible
  - can allow additional interactions
- *vibrational overtones* $\rightarrow$ transitions where $|\Delta v| > 1$
- *combination bands* $\rightarrow$ multiple excitations
- *Fermi resonances* $\rightarrow$ coupling of vibrational bands with overtones or combination bands
  - mode mixing = $\tilde{\nu}_{1,0,0} \Leftrightarrow \tilde{\nu}_{0,1,0}$
  - Fermi resonance = $\tilde{\nu}_{1,0,0} \Leftrightarrow \tilde{\nu}_{0,0,2}$
  - the two states must still have same symmetry to mix!

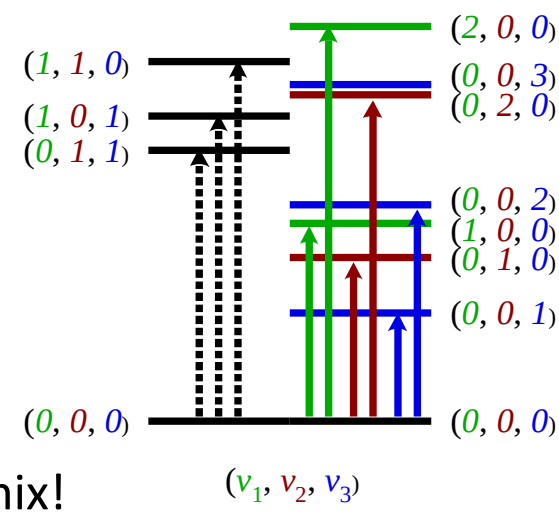

1.3 Vibrational Spectroscopy

Fermi Resonance in CO_2

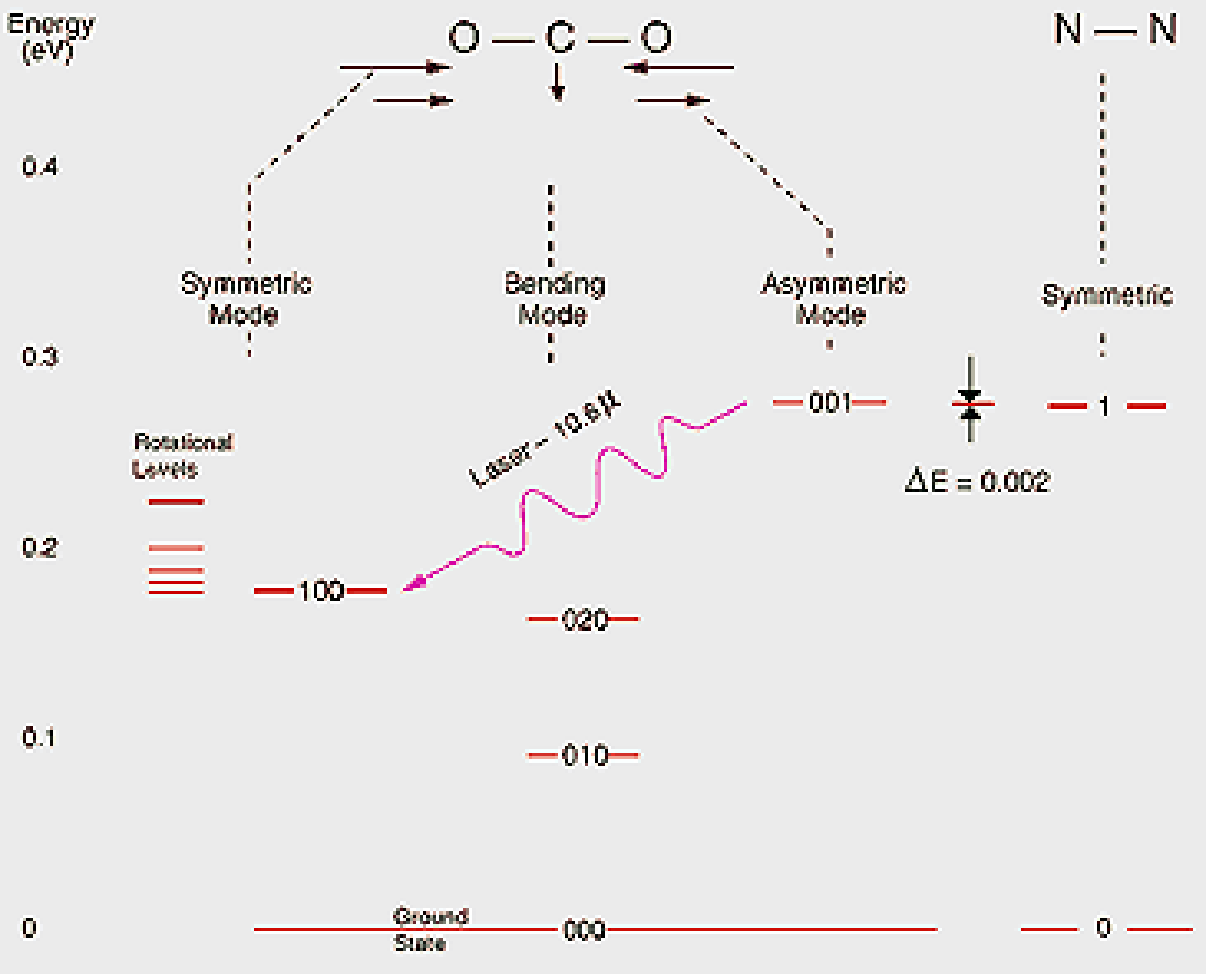

Time resolution of IR experiment

- from energy of transitions, we can easily determine frequency of oscillation for the process of interest…
  - in the infrared → $10^{12} – 10^{15}$ s^{-1} or time for single oscillation is in the *ps-fs* regime
  - compare with NMR → *nanoseconds* at best but practical limit is generally 10^{-5} seconds
  - and even EPR → theoretical limit is in hundreds of picoseconds (usable in 10^{-5}-10^{-10} *s*)

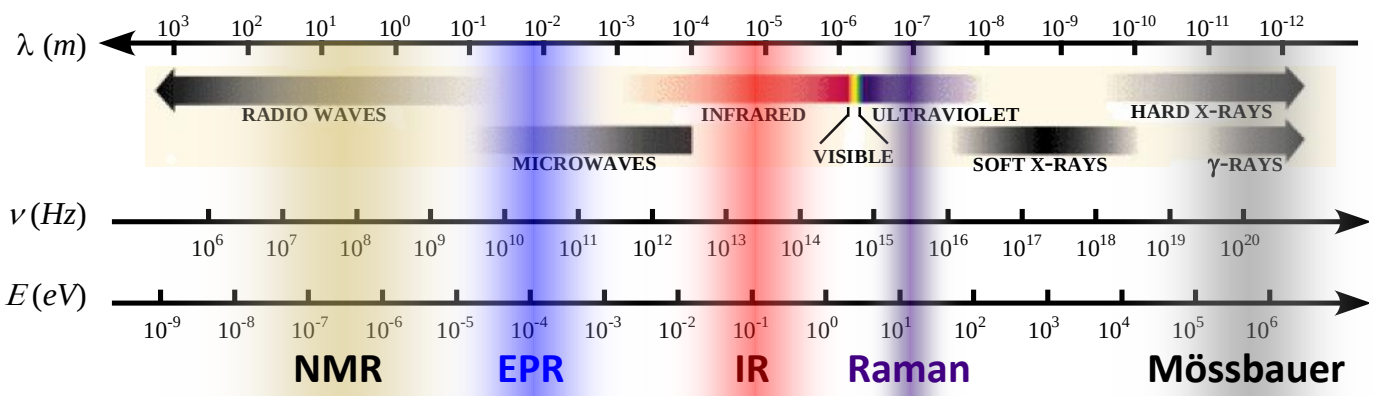

- for CO stretch…

$$E = \frac{hc}{\lambda} = \frac{h\omega}{2\pi} \rightarrow \underbrace{\omega = \frac{2\pi c}{\lambda} = 2\pi c\tilde{\nu}}_{\omega = 3.8\times10^{14}\,Hz} \qquad period = 2.64\times10^{-15}\,s = \boxed{2.64\,fs}$$

Raman vs. IR Spectroscopy

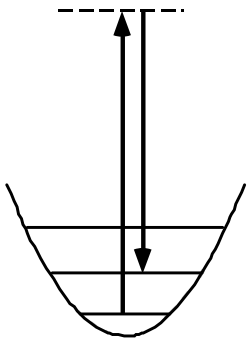

- information content is essentially identical
  - energy of vibrational modes $\rightarrow$ force constants
  - mechanical coupling of vibrational modes
- major difference $\rightarrow$ intensity mechanism/selection rules
  - for all scattering processes (Rayleigh and Raman scattering)
    - photon doesn't interact with static molecular dipole moment
    - interacts with the *induced dipole moment* caused by the electric field
    - phenomenologically $\rightarrow$ energy of molecule depends on electric field (*F*)
      - energy dependence can be expanded as a factorial series

$$
\begin{aligned}
E\ \ \vec{F} &= qE^0 + \left(\frac{\partial E}{\partial F}\right)_0 \vec{F} + \tfrac{1}{2}\left(\frac{\partial^2 E}{\partial F^2}\right)_0 \vec{F}^2 + \tfrac{1}{3!}\left(\frac{\partial^3 E}{\partial F^3}\right)_0 \vec{F}^3 + \tfrac{1}{4!}\left(\frac{\partial^4 E}{\partial F^4}\right)_0 \vec{F}^4 + \ldots \\
&= qE^0 - \mu_F \vec{F} - \tfrac{1}{2}\alpha_{FF}\vec{F}^2 - \tfrac{1}{3!}\beta_{FFF}\vec{F}^3 - \tfrac{1}{4!}\gamma_{FFFF}\vec{F}^4 - \ldots
\end{aligned}
$$

1.3 Vibrational Spectroscopy

$$E\ \vec{F} = qE^0 + \left(\frac{\partial E}{\partial F}\right)_0 \vec{F} + \tfrac{1}{2}\left(\frac{\partial^2 E}{\partial F^2}\right)_0 \vec{F}^2 + \tfrac{1}{3!}\left(\frac{\partial^3 E}{\partial F^3}\right)_0 \vec{F}^3 + \tfrac{1}{4!}\left(\frac{\partial^4 E}{\partial F^4}\right)_0 \vec{F}^4 + \ldots$$

$$= qE^0 - \mu_F \vec{F} - \tfrac{1}{2}\alpha_{FF}\vec{F}^2 - \tfrac{1}{3!}\beta_{FFF}\vec{F}^3 - \tfrac{1}{4!}\gamma_{FFFF}\vec{F}^4 - \ldots$$

electric monopole
molecular charge

electric dipole
molecular dipole moment

electric quadrupole
molecular polarizability → a.k.a. *induced dipole moment*

first-order hyperpolarizability

second-order hyperpolarizability

1.3 Vibrational Spectroscopy

- molecular dipole moment in an electric field → $\mu\ \vec{F} = \mu_0 + \underbrace{\alpha\vec{F}}_{\mu_{in}} + \ldots$
  - the polarizability (α) is the first-order *induced* dipole moment
  - β_{FFF} defines the second-order induced dipole moment, *etc.* (very small)
  - in our case – the electric field is going to be incident photons from a laser
- effect of vibrations on molecular polarizability

$$\alpha = \alpha_0 + \sum_{i=1}^{i=N} \frac{\partial \alpha}{\partial Q_i} \Delta Q_i$$

  - α will change as a function of the geometric changes
    - geometric changes defined by normal modes
  - oscillatory behaviour of coordinates can be described as $\Delta Q_i = Q_{\max} \cos\ 2\pi\nu t$
  - electric dipole part of incident EMR is also oscillatory → $\vec{F} = F_{\max} \cos\ 2\pi\nu_{ex} t$
  - therefore we can rewrite the induced dipole moment as follows...

$$\begin{aligned}\mu_{in} &= \alpha\vec{F} \\ &= \alpha_0\vec{F} + \frac{\partial \alpha}{\partial Q_1}\Delta Q_1\vec{F} + \ldots + \frac{\partial \alpha}{\partial Q_N}\Delta Q_N\vec{F} \\ &= \ldots\end{aligned}$$

continued...

1.3 Vibrational Spectroscopy

$$\cos a \times \cos b = \tfrac{1}{2}\left[\cos\left(a+b\right) + \cos\left(a-b\right)\right]$$

$$\mu_{in} = \alpha \vec{F}$$

$$= \alpha_0 \vec{F} + \frac{\partial \alpha}{\partial Q_1} \Delta Q_1 \vec{F} + \ldots + \frac{\partial \alpha}{\partial Q_N} \Delta Q_N \vec{F} = \alpha_0 \vec{F} + \sum_{i=1}^{N} \left(\frac{\partial \alpha}{\partial Q_i} \right) Q_i \vec{F}$$

$$= \alpha_0 \left[F_{\max} \cos\left(2\pi \nu_{ex} t\right) \right] + \frac{\partial \alpha}{\partial Q_1} \left[Q_1^{\max} \cos\left(2\pi \nu_1 t\right) \right] \left[F_{\max} \cos\left(2\pi \nu_{ex} t\right) \right] + \ldots + \frac{\partial \alpha}{\partial Q_N} \left[Q_N^{\max} \cos\left(2\pi \nu_N t\right) \right] \left[F_{\max} \cos\left(2\pi \nu_{ex} t\right) \right]$$

$$= \alpha_0 F_{\max} \left[\cos\left(2\pi \nu_{ex} t\right) \right] + Q_1^{\max} F_{\max} \left(\frac{\partial \alpha}{\partial Q_1} \right) \left[\cos\left(2\pi \nu_1 t\right) \cos\left(2\pi \nu_{ex} t\right) \right] + \ldots + Q_N^{\max} F_{\max} \left(\frac{\partial \alpha}{\partial Q_N} \right) \left[\cos\left(2\pi \nu_N t\right) \cos\left(2\pi \nu_{ex} t\right) \right]$$

$$= \alpha_0 F_{\max} \left[\cos\left(2\pi \nu_{ex} t\right) \right] + \tfrac{1}{2} F_{\max} \sum_{i=1}^{N} Q_i^{\max} \left(\frac{\partial \alpha}{\partial Q_i} \right) \left[\cos\left(2\pi t \left(\nu_{ex} + \nu_i\right)\right) + \cos\left(2\pi t \left(\nu_{ex} - \nu_i\right)\right) \right]$$

- look at simplified induced dipole equation...

frequency of vibrational modes

$$\mu_{in} = k_0 \left[\cos\left(2\pi \nu_{ex} t\right) \right] + \sum_{i=1}^{N} k_i \left[\cos\left(2\pi t \left(\nu_{ex} + \nu_i\right)\right) + \cos\left(2\pi t \left(\nu_{ex} - \nu_i\right)\right) \right]$$

oscillates at frequency of the incident photon: *Rayleigh scattering*

oscillates at higher frequency than photon: *Raman scattering (Anti-Stokes)*

oscillates at lower frequency than photon: *Raman scattering (Stokes)*

$$\left\langle \psi_{v=0} \middle| \hat{\mu} \middle| \psi_{v=1} \right\rangle = \left\langle \psi_{v=0} \middle| \hat{\mu}_0 + \hat{\mu}_{in} \middle| \psi_{v=1} \right\rangle = \underbrace{\left\langle \psi_{v=0} \middle| \hat{\mu}_0 \middle| \psi_{v=1} \right\rangle}_{Absorption} + \underbrace{\left\langle \psi_{v=0} \middle| \hat{\mu}_{in} \middle| \psi_{v=1} \right\rangle}_{Scattering}$$

A New Type of Secondary Radiation

C. V. Raman and K. S. Krishnan, Nature, *121(3048)*, 501, March 31, 1928

If we assume that the X-ray scattering of the 'unmodified' type observed by Prof. Compton corresponds to the normal or average state of the atoms and molecules, while the 'modified' scattering of altered wave-length corresponds to their fluctuations from that state, it would follow that we should expect also in the case of ordinary light two types of scattering, one determined by the normal optical properties of the atoms or molecules, and another representing the effect of their fluctuations from their normal state. It accordingly becomes necessary to test whether this is actually the case. The experiments we have made have confirmed this anticipation, and shown that in every case in which light is scattered by the molecules in dust-free liquids or gases, the diffuse radiation of the ordinary kind, having the same wave-length as the incident beam, is accompanied by a modified scattered radiation of degraded frequency.

The new type of light scattering discovered by us naturally requires very powerful illumination for its observation. In our experiments, a beam of sunlight was converged successively by a telescope objective of 18 cm. aperture and 230 cm. focal length, and by a second lens was placed the scattering material, which is either a liquid (carefully purified by repeated distillation *in vacuo*) or its dust-free vapour. To detect the presence of a modified scattered radiation, the method of complementary light-filters was used. A blue-violet filter, when coupled with a yellow-green filter and placed in the incident light, completely extinguished the track of the light through the liquid or vapour. The reappearance of the track when the yellow filter is transferred to a place between it and the observer's eye is proof of the existence of a modified scattered radiation. Spectroscopic confirmation is also available.

Some sixty different common liquids have been examined in this way, and every one of them showed the effect in greater or less degree. That the effect is a true scattering, and secondly by its polarisation, which is in many cases quite strong and comparable with the polarisation of the ordinary scattering. The investigation is naturally much more difficult in the case of gases and vapours, owing to the excessive feebleness of the effect. Nevertheless, when the vapour is of sufficient density, for example with ether or amylene, the modified scattering is readily demonstrable.

1.3 Vibrational Spectroscopy

- intensity for $Q_1(v{=}0) \rightarrow Q_1(v{=}1)$ is $I \propto \left\langle \psi_{v=1} \left| \frac{1}{2} F_{\max} Q_1^{\max} \left(\frac{\partial \alpha}{\partial Q_1} \right) \cos\ 2\pi t\ \nu_{ex} - \nu_i \right| \psi_{v=0} \right\rangle^2$
  - Stokes' shifts in scattering come from Δv = +1 (Anti-Stokes from -1)
    - anti-Stokes are much weaker $\rightarrow$ due to Boltzmann population distribution
  - intensity of Raman scattering depends on
    - energy of the vibrational mode $\rightarrow$ intensity only at $\nu_{ex} - \nu_i$
    - intensity of the incident photon beam $\rightarrow$ $\vec{F}_{\max}$
    - the magnitude of the vibrational distortion $\rightarrow$ $Q_1^{\max}$
    - the change in polarizability due to the vibrational mode $\rightarrow$ $\partial\alpha / \partial Q_i$
    - the energy of the incident radiation (*vide infra*)
  - this intensity equation is classical and time-dependent
    - can be derived in other ways to give

$$I = const(\nu_0 + \nu_{ij})^4 \sum_{\rho\sigma} \left| \mu_{\rho\sigma\ ij} \right|^2$$

$$\mu_{\rho\sigma\ ij} = \alpha_{\rho\sigma\ ij} \vec{F}$$

$$\alpha_{\rho\sigma\ ij} = \left\langle \psi_j^v \left| \alpha_{\rho\sigma}^{gg} \right| \psi_i^v \right\rangle$$

$$\alpha_{\rho\sigma}^{gg} = \sum_e \left(\frac{\left\langle \phi_g^* \left| \mu_\sigma \right| \phi_e \right\rangle \left\langle \phi_e^* \left| \mu_\rho \right| \phi_g \right\rangle}{\Delta\nu_{eg} - \nu_{ex}} + \frac{\left\langle \phi_g^* \left| \mu_\rho \right| \phi_e \right\rangle \left\langle \phi_e^* \left| \mu_\sigma \right| \phi_g \right\rangle}{\Delta\nu_{eg} + \nu_{ex}} \right)$$

$\mu_{\rho\sigma} \mapsto$ induced dipole moment (often $P_{\rho\sigma}$)
$\rho \mapsto$ direction of incident photon (x, y, z)
$\sigma \mapsto$ direction of scattered photon (x, y, z)
$i, j \mapsto$ vibrational quantum numbers in GS
$\nu_{ex} \mapsto$ vibrational quantum numbers in GS

Selection Rules for Raman Spectroscopy → $I \propto \left\langle \psi_j^v \middle| \alpha_{\rho\sigma}^{gg} \middle| \psi_i^v \right\rangle^2$

- vibrational quantum number → $j = i \pm 1 \quad \mapsto \quad \Delta v = \pm 1$
- vibrational normal modes → $\alpha_{\rho\sigma}^{gg} \mapsto \text{quadratic functions } (x^2, y^2, z^2, xy, xz, yz)$
  - use symmetry of vibrational modes (*from IR section*)

$$\Psi_0 \propto \psi_0^{q_1} \quad \psi_0^{q_2} \quad \psi_0^{q_3} \ldots \rightarrow A_1 \quad A_1 \quad A_1 \ldots \rightarrow A_1$$

$$\Psi_1 \propto \psi_1^{q_1} \quad \psi_0^{q_2} \quad \psi_0^{q_3} \ldots \rightarrow \Gamma_{q_1} \quad A_1 \quad A_1 \ldots \rightarrow \Gamma_{q_1}$$

$$\left\langle \psi_0^v \middle| \alpha_{\rho\sigma}^{gg} \middle| \psi_1^v \right\rangle \mapsto \Gamma_{v=0} \times \Gamma_\alpha \times \Gamma_{v=1}$$

$$\mapsto \underline{\Gamma_\alpha \times \Gamma_{q_1}}$$

symmetry of vibrational mode must be the same as at least one of the quadratic functions

- *e.g.*, allowed Raman transitions for H_2O

C_{2v}	E	C_2	σ_{xz}	σ_{yz}	
A_1	+1	+1	+1	+1	z, x^2, y^2, z^2
A_2	+1	+1	-1	-1	R_z, xy
B_1	+1	-1	+1	-1	x, R_y, xz
B_2	+1	-1	-1	+1	y, R_x, yz

$$S_{A_1} = \frac{1}{\sqrt{2}}(\Delta r_1 + \Delta r_2)$$

$$S_{B_1} = \frac{1}{\sqrt{2}}(\Delta r_1 - \Delta r_2)$$

$$S_{A_1} = \Delta\theta$$

all allowed!

1.3 Vibrational Spectroscopy

- what about $[NO_3]^-$?
  - remember that not all vibrational modes were allowed in infrared absorption...

D_{3h}	E	$2C_3$	$3C_2$	σ_h	$2S_3$	$3\sigma_v$	
A_1'	1	1	1	1	1	1	x^2+y^2, z^2
A_2'	1	1	-1	1	1	-1	R_z
E'	2	-1	0	2	-1	0	(x,y), (x^2-y^2,xy)
A_1''	1	1	1	-1	-1	-1	
A_2''	1	1	-1	-1	-1	1	z
E''	2	-1	0	-2	1	0	(R_x,R_y), (xz,yz)

			IR	Raman
$A_1' \mapsto$	$S^{\Delta r}_{A_1'} = \frac{1}{\sqrt{3}}\ \Delta r_1 + \Delta r_2 + \Delta r_3$	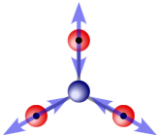	-	x^2+y^2, z^2
$E' \mapsto$	$S^{\Delta\vec{r}}_{E'}(1) = \frac{1}{\sqrt{6}}\ 2\Delta\vec{r}_1 - \Delta\vec{r}_2 - \Delta\vec{r}_3$ $S^{\Delta\vec{r}}_{E'}(2) = \frac{1}{\sqrt{2}}\ \Delta\vec{r}_2 - \Delta\vec{r}_3$		(x,y)	(x^2-y^2,xy)
$E' \mapsto$	$S^{\Delta\vec{\theta}}_{E'}(1) = \frac{1}{\sqrt{6}}\ 2\Delta\vec{\theta}_1 - \Delta\vec{\theta}_2 - \Delta\vec{\theta}_3$ $S^{\Delta r}_{E'}(2) = \frac{1}{\sqrt{2}}\ \Delta\vec{\theta}_2 - \Delta\vec{\theta}_3$	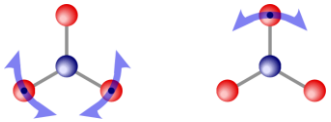	(x,y)	(x^2-y^2,xy)
$A_2'' \mapsto$	$S^{\Delta\vec{\phi}}_{A_2''} = \frac{1}{\sqrt{3}}\ \Delta\vec{\phi}_1 + \Delta\vec{\phi}_2 + \Delta\vec{\phi}_3$	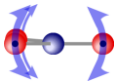	z	-

Transition polarisation in Raman Spectroscopy

- a.k.a. *Raman Depolarisation Ratios*
- more complicated since we are now looking at tensors not vectors!
  - cannot directly detect polarization directions
  - *linear polarizer* to measure contributions from two perpendicular directions
    - for a *z*-polarized excitation laser coming from the *y*-direction and measuring along the *x*-direction → $I_{tot} = I_y + I_z \propto \alpha_{yz}^2 \vec{F}_z^2 + \alpha_{zz}^2 \vec{F}_z^2$
    - define depolarisation ratio as $\rho = \frac{I_y}{I_z} = \frac{\alpha_{yz}^2 \vec{F}_z^2}{\alpha_{zz}^2 \vec{F}_z^2}$
- ratio depends on symmetry of vibrations
  - totally symmetric → $0 \leq \rho < 0.75$ polarised
  - asymmetric → depolarised $\rho \geq 0.75$
  - predicted by group theory...

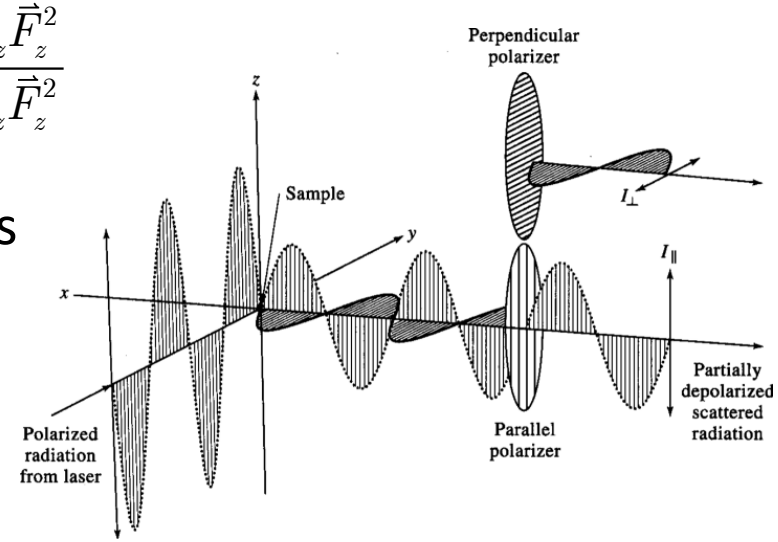

Resonance Raman Spectroscopy

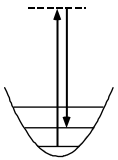

- we have considered the information content of "off-resonance" processes
  - excitation occurs to a *virtual* excited state → coupling is very weak (intensity is low)
- look back at intensity equation → $\alpha_{\rho\sigma\ ij} = \left\langle \psi_j^v \middle| \alpha_{\rho\sigma}^{gg} \middle| \psi_i^v \right\rangle$
  - depends on coupling with real excited states! (but coupling is poor)
  - but what happens if coupling is strong?
    - *resonance enhancement!!!!*

$$\alpha_{\rho\sigma}^{gg} = \sum_e \left(\frac{\left\langle \phi_g^* \middle| \mu_\sigma \middle| \phi_e \right\rangle \left\langle \phi_e^* \middle| \mu_\rho \middle| \phi_g \right\rangle}{\Delta\nu_{eg} - \nu_{ex}} + \frac{\left\langle \phi_g^* \middle| \mu_\rho \middle| \phi_e \right\rangle \left\langle \phi_e^* \middle| \mu_\sigma \middle| \phi_g \right\rangle}{\Delta\nu_{eg} + \nu_{ex}} \right)$$

denominator → 0

this term → ∞

these equations fail *on* resonance – need to include lifetime of final state

- Resonance Raman dramatically improves the sensitivity of vibrational modes
  - off-resonance probability of inelastic scattering ~ 10^{-6}-10^{-7}
  - on-resonance probability of inelastic scattering ~ 10^{-3}-10^{-1}

  $10^3 – 10^6$ enhancement!
  - important → selective enhancement that depends on the nature of excited state
    - only if excited state increases magnitude of specific induced dipole (along Q_i)
    - this means that only excited states that *are coupled with* the vibrational mode will be enhanced

      e.g. enhancement of an M-X vibration will occur if laser hits X→M LMCT band

Case Study: IR spectroscopy in Organometallic Photochemistry

Organometallics **1996**, *15*, 604−614

Photocatalytic Hydrosilylation of Conjugated Dienes with Triethylsilane in the Presence of $Cr(CO)_6$

Wafa Abdelqader,† Dietmar Chmielewski,‡ Friedrich-Wilhelm Grevels,*,‡ Saim Özkar,*,† and Nihad Bekir Peynircioglu†

Department of Chemistry, Middle East Technical University, 06531 Ankara, Turkey, and Max-Planck-Institut für Strahlenchemie, Postfach 101365, D-45413 Mülheim an der Ruhr, Germany

Chromium carbonyl photocatalyzed hydrosilylation of 1,3-butadiene, *trans*-1,3-pentadiene, 2,3-dimethyl-1,3-butadiene, 2-methyl-1,3-butadiene, *trans*-2-methyl-1,3-pentadiene, and 1,3-cyclohexadiene with triethylsilane yields the *cis*-1,4-adducts, 1-(triethylsilyl)-2-butene derivatives, as the main products which have been isolated by distillation or preparative GC and fully characterized by NMR spectroscopy. The proposed mechanism involves the initial conversion of $Cr(CO)_6$ into $Cr(CO)_4(\eta^4$-1,3-diene) followed by a further photolytic CO substitution by triethylsilane forming a $Cr(CO)_3(H)(SiEt_3)(\eta^4$-1,3-diene) intermediate. Experiments with $D-SiEt_3$ lead to the conclusion that reversible addition of the hydride to the diene with formation of an η^3-enyl intermediate occurs prior to the irreversible silyl transfer to the organic moiety. The 1,4-hydrosilylation adduct is then replaced by new substrates to complete the catalytic cycle.

1.3 Vibrational Spectroscopy

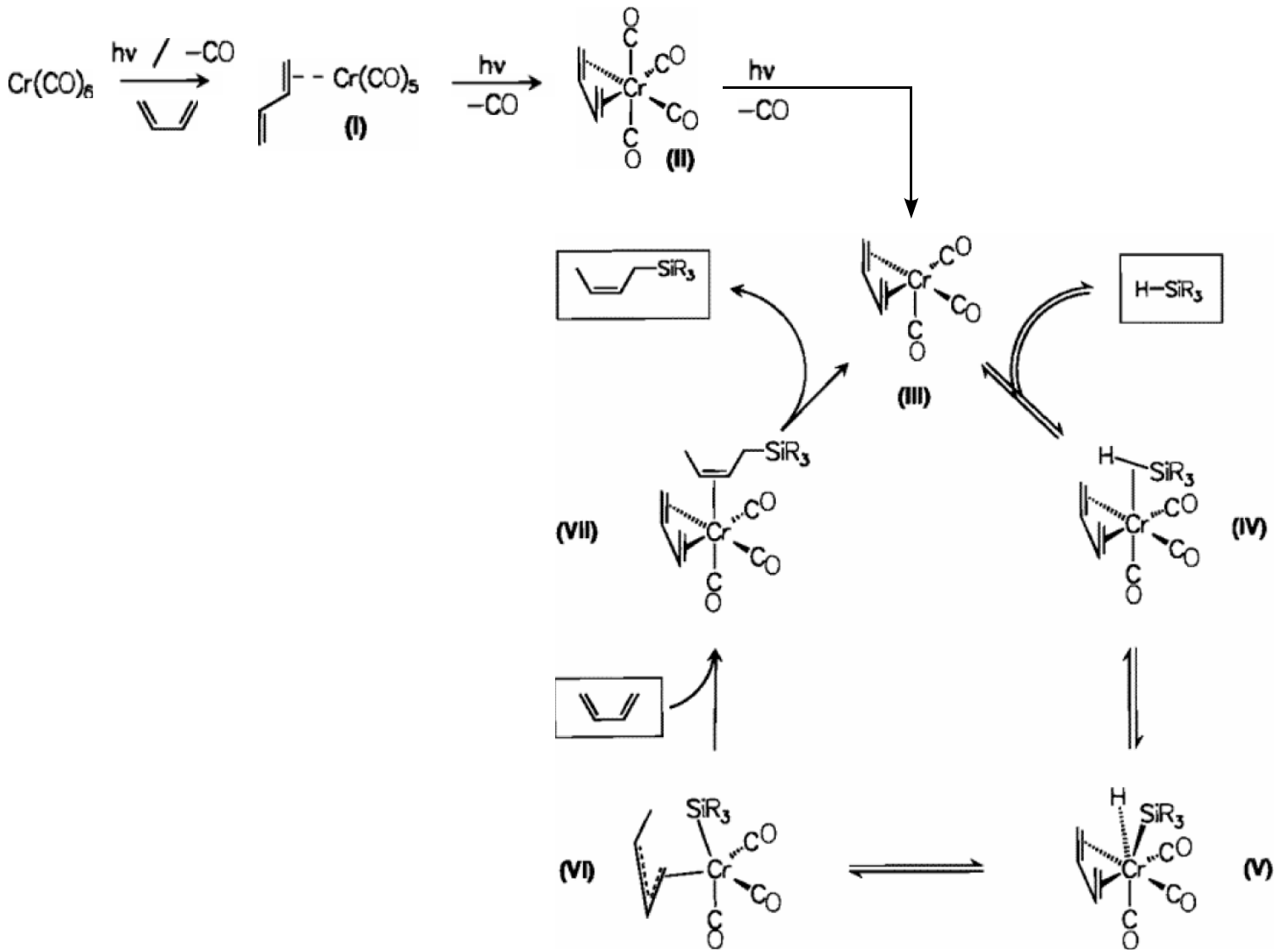

1.3 Vibrational Spectroscopy

J. Am. Chem. Soc. **1998,** *120,* 10423−10433

The Very Low Barrier of CO Site Exchange in Tricarbonyl(η^4-1,5-cyclooctadiene)iron: Picosecond Kinetics in Solution Investigated by Line Shape Simulation of the ν(CO) IR Bands and Complementary Evidence from the Course of ^{13}CO Incorporation in a Low-Temperature Matrix

Friedrich-Wilhelm Grevels,*,† Klaus Kerpen,† Werner E. Klotzbücher,† R. E. D. McClung,*,‡ Graham Russell,† Manuella Viotte,† and Kurt Schaffner†

Contribution from the Max-Planck-Institut für Strahlenchemie, D-45413 Mülheim an der Ruhr, Germany, and the Department of Chemistry, University of Alberta, Edmonton, AB T6G 2G2, Canada

Received November 13, 1997

Abstract: Photochemical experiments with Fe(CO)$_3$(η^4-1,5-cyclooctadiene) (**1**) in a ^{13}CO matrix at 10 K, monitored by means of IR spectroscopy, indicate the generation of stereoselectively labeled Fe(CO)$_2$(^{13}CO)-(η^4-1,5-cyclooctadiene) (**1**-*1a*), with ^{13}CO in the apical position of the square-pyramidal coordination geometry. The spectral changes occurring upon annealing the matrix to 28 K reveal the thermally activated conversion into a mixture of the two possible stereoisotopomers, the species with ^{13}CO in a basal position (**1**-*1b*) becoming predominant. These findings characterize the carbonyl ligand site exchange in complex **1** as a chemical reaction involving a very small barrier. The variable-temperature IR spectra of **1** in hydrocarbon solution exhibit broadening and coalescence of bands in the ν(CO) region, which is interpreted in terms of a CO site exchange occurring in the picosecond time domain. The theoretical approach to the simulation of these spectral changes involves a transfer of transition dipole moment between the ν(CO) modes. On the basis of this approach, the rates of CO site exchange at the various temperatures could be evaluated by line shape simulation. They were found to range from 0.15×10^{12} s^{-1} at 133 K to 1.54×10^{12} s^{-1} at 293 K, yielding $\Delta H^{\ddagger} = 0.7$ kcal·mol^{-1} (Eyring plot) and $E_a = 1.1$ kcal·mol^{-1} (Arrhenius plot) for the activation barrier of the underlying process.

1.3 Vibrational Spectroscopy

Broadening and coalescence of CO stretching vibrational bands has been observed in the variable-temperature IR spectra of the tricarbonyl(η^4-diene)iron complexes **1** (diene = 1,5-cyclooctadiene; 1,5-cod) and **2** (diene = norbornadiene; nbd) and a few other, related compounds.[1−5]

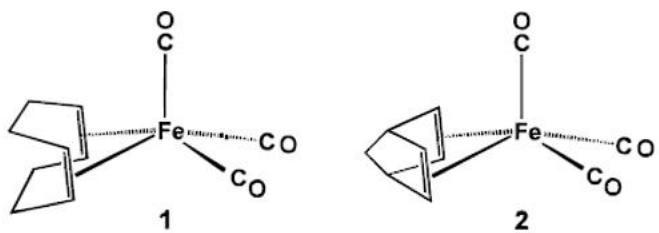

These spectral changes, illustrated in Figure 1 for the example of the norbornadiene complex **2**,[2] were interpreted in terms of a low-barrier, very fast site exchange of the CO ligands[6] in the apical and basal positions of the square-pyramidal coordination geometry, presumably proceeding via the turnstile rotation mechanism. In support of this notion, the temperature dependent changes in the ν(CO) pattern of a ^{13}CO-enriched[7] sample[4] of **2** proved consistent with an equally rapid interconversion of positional isotopomers (CO/^{13}CO site exchange), as sketched out in Scheme 1 for the case of the monolabeled species Fe(CO)$_2$(^{13}CO)(η^4-nbd) carrying the ^{13}CO group in the apical (**2**-*1a*) or a basal (**2**-*1b*/**2**-*1b*′) position.[7]

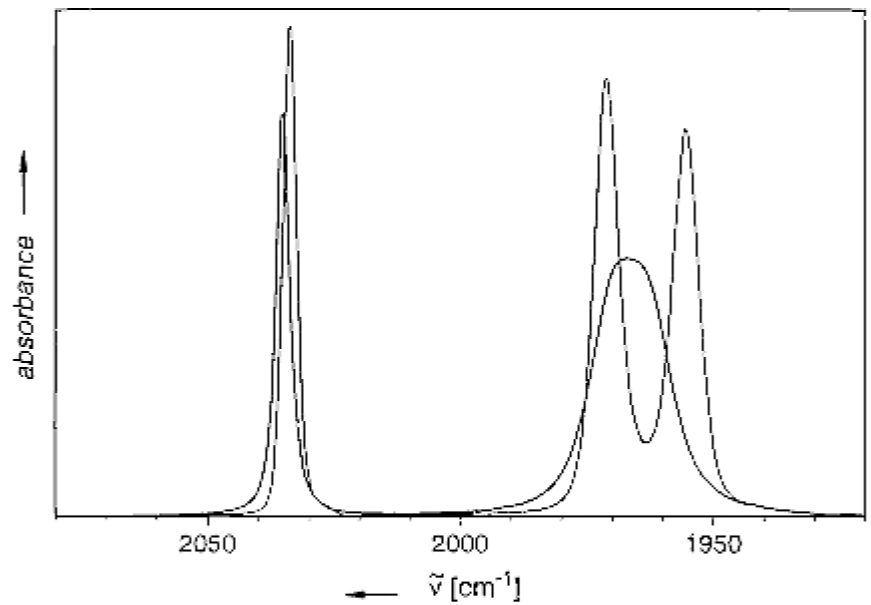

Figure 1. The ν(CO) bands in the IR spectrum of Fe(CO)$_3$(η^4-nbd) (**2**) recorded in 2-methylpentane solution[2] at 293 K (bold line) and 133 K

1.3 Vibrational Spectroscopy

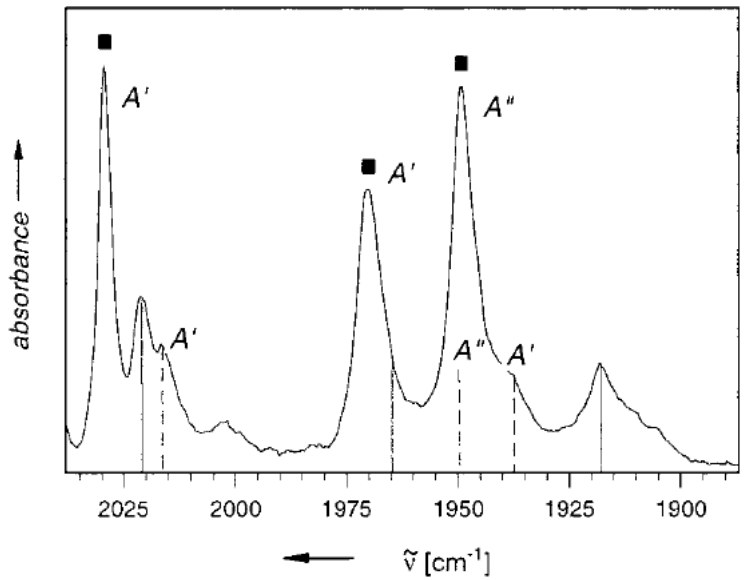

Figure 2. The ν(CO) bands in the IR spectrum of $Fe(CO)_{3-n}(^{13}CO)_n$-(η^4-1,5-cod) (**1**-#; $n = 0$, 54%; $n = 1$, 37%; $n = 2$, 8%)[21] recorded in a ^{13}CO matrix at 10 K. The symbols and vertical lines, respectively, refer to the unlabeled complex **1** (■) and to the two monolabeled positional isotopomers **1**-*1a* (- - -) and **1**-*1b* (—) carrying the ^{13}CO label in the apical or a basal position (cf. Table 1).

Table 1. The CO Stretching Vibrations of $Fe(CO)_3(\eta^4$-1,5-cod) (**1**) and Its ^{13}CO Monolabeled Isotopomers in the IR Spectrum of a Statistically ^{13}CO-Enriched Sample (1-#)[7,21] Recorded in a ^{13}CO Matrix at 10 K

complex	$\tilde{\nu}$(CO) [cm^{-1}] obsd	calcd[b]	ν(CO) normal coordinates[a]
1 (C_s)	2029.5	2029.7	Q_1 (A') = $0.6659r_1 + 0.5275r_2 + 0.5275r_3$
	1970.2	1970.3	Q_2 (A') = $0.7461r_1 - 0.4708r_2 - 0.4708r_3$
	1949.5	1949.8	Q_3 (A'') = $0.7071r_2 - 0.7071r_3$
1-*1a* (C_s)	2016.4	2016.4	Q_1 (A') = $0.4080r_1 + 0.6456r_2 + 0.6456r_3$
	(—)[c]	1949.8	Q_2 (A'') = $-0.7071r_2 + 0.7071r_3$
	(—)[c]	1938.1	Q_3 (A') = $0.9130r_1 - 0.2885r_2 - 0.2885r_3$
1-*1b* (C_1)[d]	2021.3	2021.2	Q_1 (A) = $0.7586r_1 + 0.3389r_2 + 0.5564r_3$
	(—)[c]	1965.7	Q_2 (A) = $-0.6353r_1 + 0.1953r_2 + 0.7472r_3$
	1918.1	1917.8	Q_3 (A) = $-0.1446r_1 + 0.9203r_2 - 0.3635r_3$
1-*1b'* (C_1)[e]	2021.3	2021.2	Q_1 (A) = $0.7586r_1 + 0.5564r_2 + 0.3389r_3$
	(—)[c]	1965.7	Q_2 (A) = $-0.6353r_1 + 0.7472r_2 + 0.1953r_3$
	1918.1	1917.8	Q_3 (A) = $-0.1446r_1 - 0.3635r_2 + 0.9203r_3$

[a] Notations r_1, r_2, and r_3 refer to the internal CO stretching coordinates in positions 1 (apical), 2 (basal), and 3 (basal). [b] CO force field parameters: $k_a = 1610.3$, $k_b = 1578.2$, $k_{ab} = 33.7$, $k_{bb} = 43.0$ N m^{-1}; the effective value for $\sqrt{\mu(^{12}C^{16}O)/\mu(^{13}C^{16}O)} = 0.9772$, employed in this calculation, is adopted from $Fe(CO)_3(\eta^4$-1,3-butadiene).[42] [c] Blank entries refer to bands hidden underneath more prominent absorptions. [d] ^{13}CO label in position 2. [e] ^{13}CO label in position 3.

1.3 Vibrational Spectroscopy

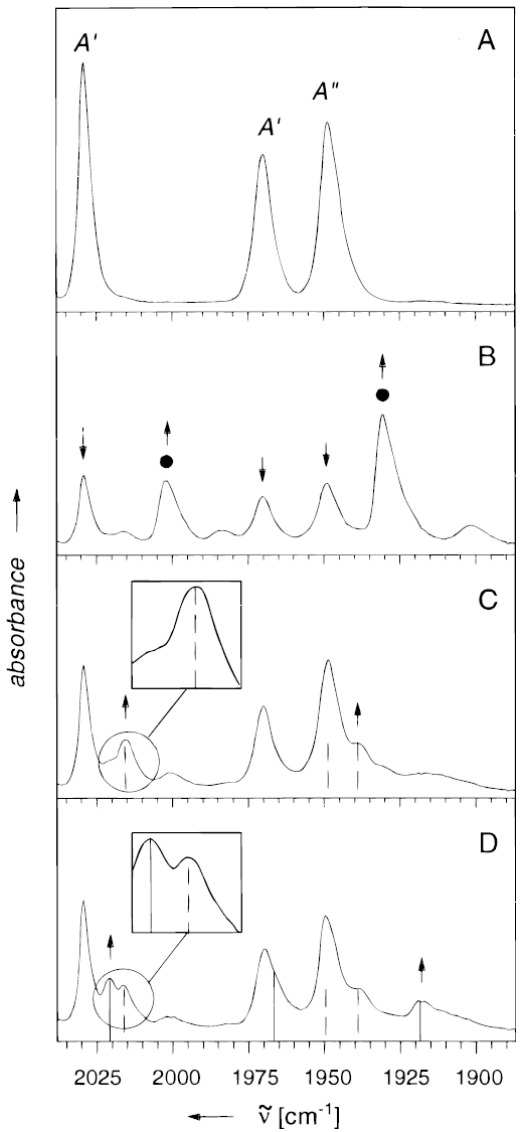

Figure 3. IR spectra in the ν(CO) region from an experiment with $Fe(CO)_3(\eta^4$-1,5-cod) (**1**) in a ^{13}CO matrix. (A) After deposition at 10 K. (B) After irradiation at λ_{exc} = 365 nm for 20 min, generating the $Fe(CO)_2(\eta^4$-1,5-cod) fragment (**3**, ●). (C) After subsequent irradiation through a 495 nm cutoff filter for 2 min, leading to incorporation of ^{13}CO with formation of apically labeled $Fe(CO)_2(^{13}CO)(\eta^4$-1,5-cod) (**1**-*1a*, - - -). (D) After subsequent annealing of the matrix to 28 K, indicating the appearance of the positional isotopomer **1**-*1b* (—). Arrows indicate the most significant changes in intensity.

Scheme 3

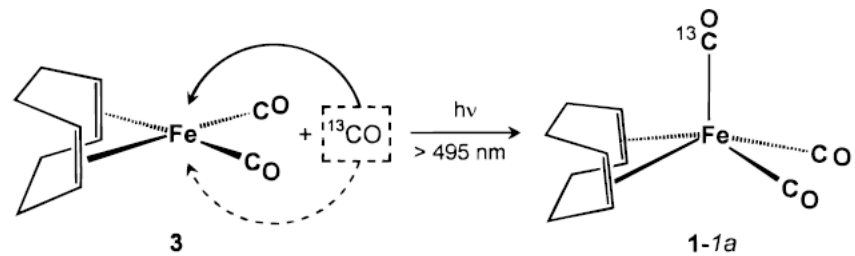

Scheme 4

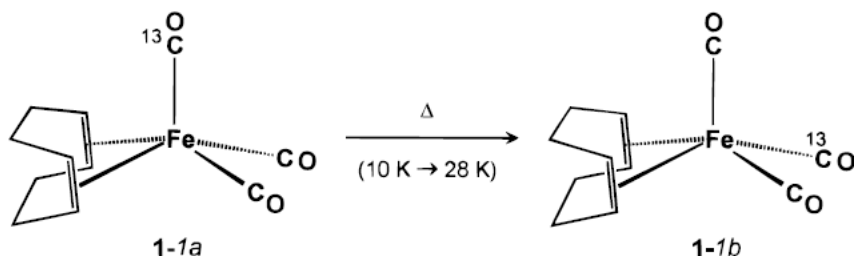

1.3 Vibrational Spectroscopy

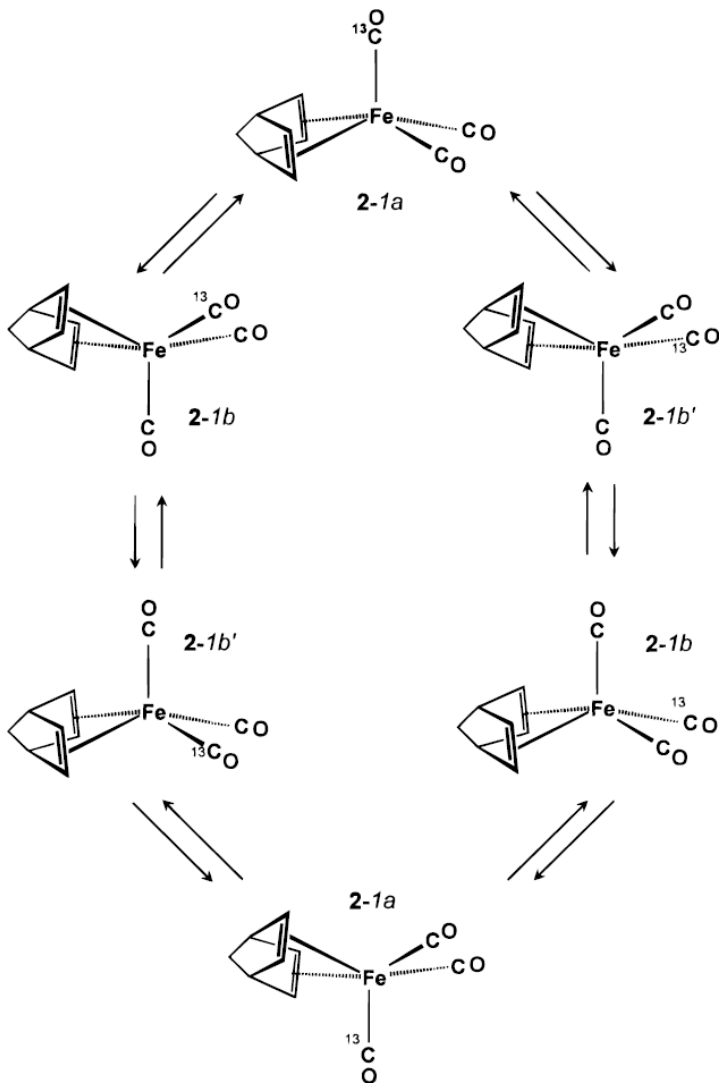

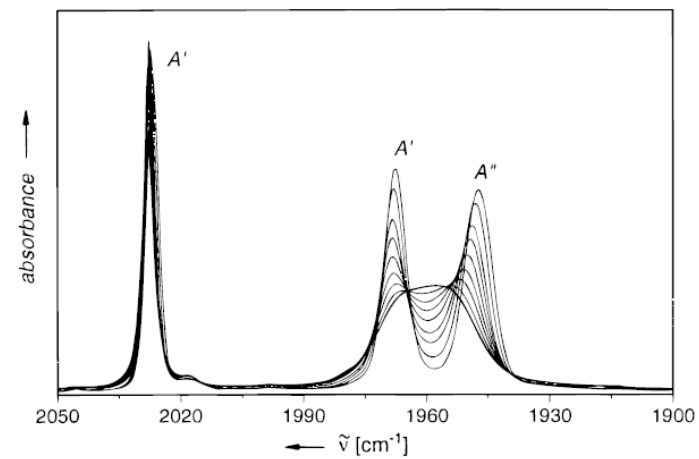

Figure 4. The ν(CO) bands in the variable-temperature IR spectra of $Fe(CO)_3(\eta^4$-1,5-cod) (**1**), recorded in 2-methylpentane solution at 293 K (bold line) and 273/253/233/213/193/173/153/133 K.

Table 2. The CO Stretching Vibrational Bands in the IR Spectra of $Fe(CO)_3(\eta^4$-1,5-cod) (**1**), $Fe(CO)_3(\eta^4$-1,3-butadiene) (**4**), and $Fe(CO)(\eta^4$-1,3-butadiene$)_2$ (**5**), Recorded in 2-Methylpentane Solution and Analyzed by Curve Fitting[25] to the Voigt Function

complex	T [K]	$\tilde{\nu}_{max}$ [cm^{-1}]	assignment	rel intensity [%]	$\Gamma^{(L)\,a}$ [cm^{-1}]	$\Gamma^{(G)\,a}$ [cm^{-1}]
1	133	2026.9	A'	27.3	1.33	2.77
		1967.7	A'	34.6	2.82	4.51
		1947.4	A''	38.2	2.37	6.69
4	133	2055.2	A'	22.3	1.58	1.70
		1987.8	A'	42.0	1.53	3.76
		1977.3	A''	35.8	2.07	3.81
4	293	2056.1	A'	22.5	2.87	1.13
		1990.3	A'	43.8	3.76	0.98
		1980.1	A''	33.7	3.83	1.20
5	133	1983.5			1.78	6.34
5	293	1985.9			5.47	2.75

[a] Lorentzian and Gaussian line width components.

1.3 Vibrational Spectroscopy

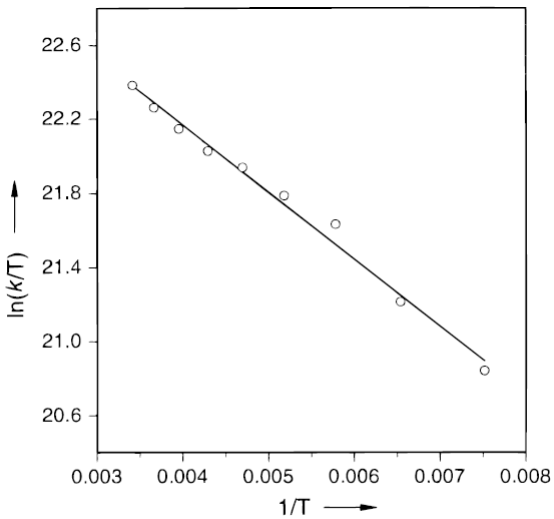

Figure 7. Eyring plot of $\ln(k/T)$ vs $1/T$ yielding $\Delta H^{\ddagger} = 0.7$ kcal·mol^{-1} and $\Delta S^{\ddagger} = -0.3$ cal·K^{-1}·mol^{-1} for the CO site exchange process in $Fe(CO)_3(\eta^4$-1,5-cod) (**1**).

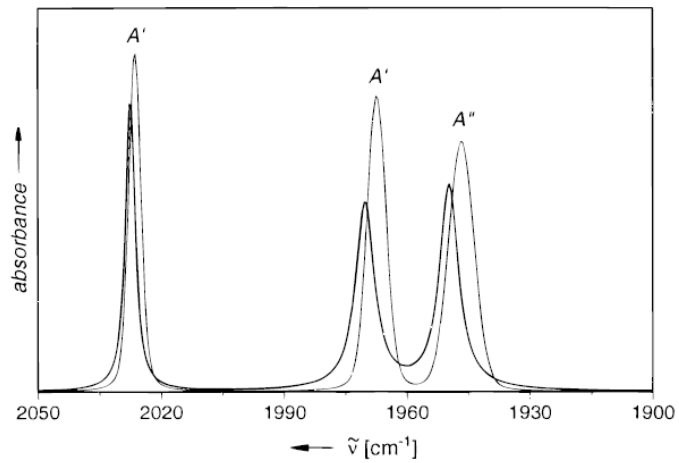

Figure 8. The hypothetical IR ν(CO) pattern of $Fe(CO)_3(\eta^4$-1,5-cod) (**1**) in the absence of CO site exchange at 293 K (bold line) and 133 K simulated with the respective spectral parameters listed in Table 3,[41] but with $k_{react} = 0$ s^{-1}.

Scheme 7

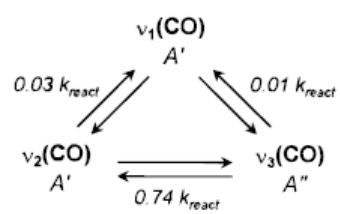

vibrational dipole moment interchange between the three ν(CO) modes of the complex is described by the matrix

$$\mathbf{K} = k_{react}(\mathbf{Z} - \mathbf{1}) = k_{react}\begin{pmatrix} -0.0378 & 0.0283 & 0.0096 \\ 0.0283 & -0.7687 & 0.7405 \\ 0.0096 & 0.7405 & -0.7500 \end{pmatrix}$$

1.3 Vibrational Spectroscopy

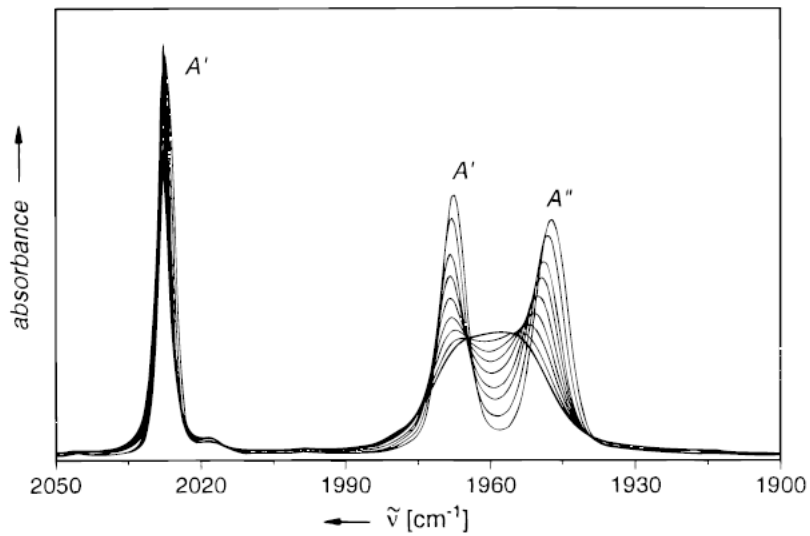

Figure 4. The ν(CO) bands in the variable-temperature IR spectra of $Fe(CO)_3(\eta^4$-1,5-cod) (**1**), recorded in 2-methylpentane solution at 293 K (bold line) and 273/253/233/213/193/173/153/133 K.

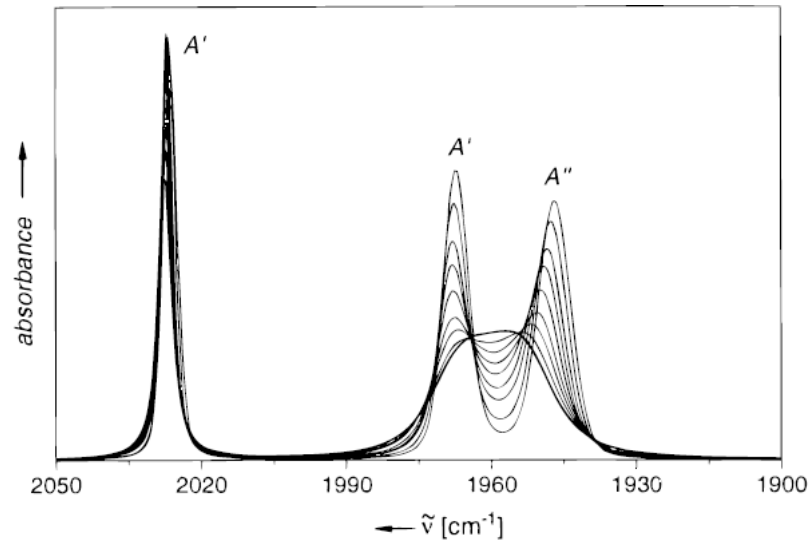

Figure 6. Simulation of the ν(CO) bands in the variable-temperature IR spectra of $Fe(CO)_3(\eta^4$-1,5-cod) (**1**), using rate constants for the CO site exchange process ranging from 1.5×10^{11} s^{-1} at 133 K to 1.54×10^{12} s^{-1} at 293 K (bold line) and spectral parameters listed in Table 3.[41]

Electron Donor–Acceptor Properties of Phosphorus Ligands. Substituent Additivity

Chadwick A. Tolman

Contribution No. 1577 from the Central Research Department, Experimental Station, E. I. du Pont de Nemours and Company, Wilmington, Delaware 19898. *Received July 14, 1969*

Abstract: A rapid method is described for determining electron donor–acceptor properties of triply connected phosphorus ligands based on the A_1 carbonyl stretching frequency of $Ni(CO)_3L$ in CH_2Cl_2. Data are given for 70 ligands and a substituent additivity rule is proposed. Forty-seven substituent parameters χ_i are derived and found to correlate well with Kabachnik's σ parameters, based on ionization constants of phosphorus acids.

ja00713a006 – C.A. Tolman, J. Am. Chem. Soc., **92**, 2953 (1970)

1.3 Vibrational Spectroscopy

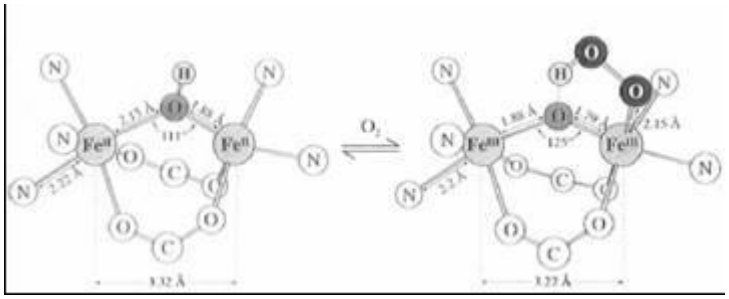

hemocyanin – oxygen carrier protein in arthropods

look at bending modes for M-O-M:

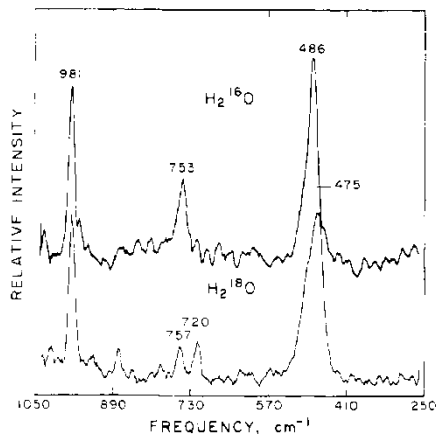

Figure 1. Resonance Raman spectrum of oxyhemerythrin in $H_2{}^{16}O$ (upper) and $H_2{}^{18}O$ (lower). Protein concentration ≈1.2 mM in monomer; 363.8-nm excitation, 20 mW; scan rate, 1.0 cm^{-1}/s; slit width, 8.0 cm^{-1}. The peak at 981 cm^{-1} is due to 0.3 M SO_4^{2-} used as an internal standard.

Table I. Vibrational Frequencies (cm^{-1}) for the Stretching and Deformation Modes of the Fe–O–Fe Cluster in Hemerythrins and Model Compounds

sample	ν_s(Fe–O–Fe)[a]		ν_{as}(Fe–O–Fe)[e]		δ(Fe–O–Fe)[a]	
	$H_2{}^{16}O$	$H_2{}^{18}O$	$H_2{}^{16}O$	$H_2{}^{18}O$	$H_2{}^{16}O$	$H_2{}^{18}O$
hemerythrin						
oxy	486	475	~753	720	n.o.	n.o.
azidomet	507	493	768	733	292	286
thiocyanatomet	514	498	780	742	~290	~285
met	510	496	~750	~715	n.o.	n.d.
hydroxomet	508	n.d.	780	~750	n.o.	n.d.
cyanatomet	509	493[f]	782	n.d.	n.o.	n.d.
cyanomet	512	499[f]	780	n.d.	n.o.	n.d.
model compound						
$Fe_2O(CH_3COO)_2(HB(pz)_3)_2$[b]	528	511	751	721	283	269
$[Fe_2O(phen)_4(H_2O)_2]^{4+}$[c]	395	390	827	788	n.o.	n.o.
$[Fe_2OCl_6]^{2-}$[d]	458	440	870	826	203	198

[a] Values obtained by Raman spectroscopy (n.d. = not determined; n.o. = not observed). The ν_s(Fe–O–Fe) values for the methemerythrins in H_2O are similar (±1 cm^{-1}) to those reported previously.[13] [b] Reference 27. [c] Reference 29. [d] Reference 26. [e] Values for hemerythrin obtained by Raman spectroscopy. Values for model compounds obtained by IR spectroscopy. Uncertainty in frequencies (indicated by ~) due to the interference of other protein peaks. [f] Reference 13.

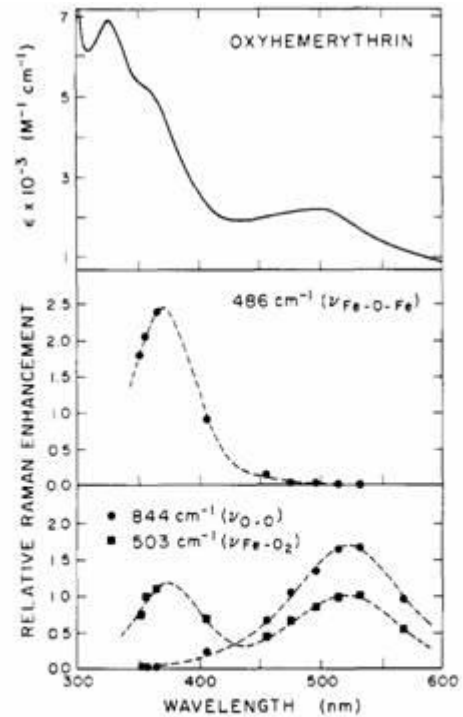

Figure 2. Resonance Raman enhancement profiles for oxyhemerythrin. (Upper) Electronic absorption spectrum of oxyhemerythrin. (Middle) Enhancement profile for the symmetric Fe–O–Fe vibration at 486 cm^{-1}. (Lower) Enhancement profiles for the vibrations of the bound peroxide: O–O stretch at 844 cm^{-1}; Fe–O_2 stretch at 503 cm^{-1}. Enhancement measured as the height of the Raman peak relative to the height of ν_1 of 0.3 M SO_4^{2-} at 981 cm^{-1} and normalized to the ν(Fe–O_2) height obtained with 530.9-nm excitation.

1.3 Vibrational Spectroscopy

$$F_S = \begin{bmatrix} k_{11} + i_{12} & \cancel{\sqrt{2}i_{13}} & 0 \\ \cancel{\sqrt{2}i_{13}} & k_{33} & 0 \\ 0 & 0 & k_{11} - i_{12} \end{bmatrix} \qquad G_S = \begin{bmatrix} \mu_1 + \mu_3(1+\cos\theta) & -\frac{\sqrt{2}\mu_3}{r}\sin\theta & 0 \\ -\frac{\sqrt{2}\mu_3}{r}\sin\theta & \frac{2}{r^2}(\mu_1 + \mu_3 - \mu_3\cos\theta) & 0 \\ 0 & 0 & \mu_1 + \mu_3(1-\cos\theta) \end{bmatrix}$$

frequencies depend on θ (at equil) because this defines i_{12} (see G_S) *due to mass not force*

$$\nu_s \;\; cm^{-1} = 1303.1\sqrt{(k_{11} + i_{12})\;\mu_M + \mu_O(1+\cos\theta)}$$

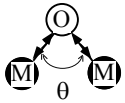

$$\nu_{as} \;\; cm^{-1} = 1303.1\sqrt{(k_{11} - i_{12})\;\mu_M + \mu_O(1-\cos\theta)}$$

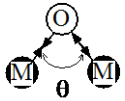

↓

can determine θ from bond stretching frequencies!

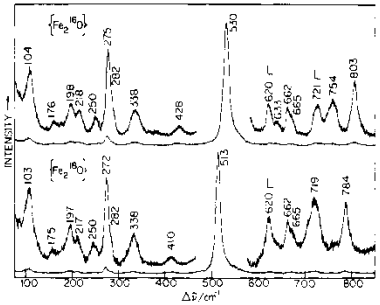

Figure 3. Low-temperature (77 K) resonance Raman spectra of crystalline $[Fe_2O(O_2CCH_3)_2(HB(pz)_3)_2]$ and its μ-^{18}O analogue obtained with 4067-Å excitation (100 mW) and 5-cm^{-1} slit width. "L" marks bands associated with internal modes of $HB(pz)_3^-$ ligands.

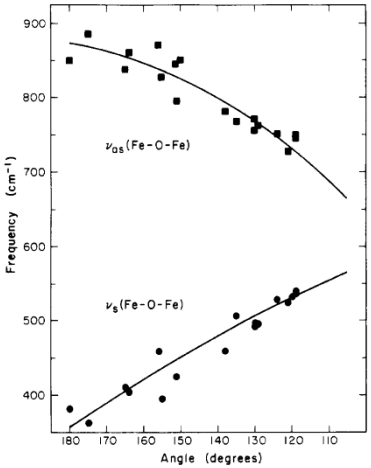

Figure 2. Correlation of vibrational frequencies for the Fe–O–Fe symmetric and asymmetric stretches with the observed Fe–O–Fe angle from Table I.

Table I. Vibrational Frequencies and Parameters of Oxo-Bridged Fe(III) Complexes

sample	Fe–O–Fe angle[a] obs	Fe–O–Fe angle[a] calc	Fe–O–Fe stretch[b] ν_s	$\Delta^{18}O$	ν_{as}	$\Delta^{18}O$	Fe–O distances[a] Fe 1	Fe 2
Monobridged Complexes								
$[Fe_2O(Cl\text{-}pdc)_2(H_2O)_4]$	180		381		850		1.77	1.77
$[Fe_2O(TPP)]$	175		363		865		1.76	1.76
$[Fe_2O(hedta)_2]^{2-}$	165	167	409	−2[c]	838		1.80	1.79
$[Fe_2O(n\text{-}propsal)_4]$	164		403		860		1.76	1.78
$[Fe_2OCl_6]^{2-}$	156		458	−18	870	−44	1.76	1.76
$[Fe_2O(phen)_4(H_2O)_2]^{4+}$	155	156	395	−5	827	−39	1.78	1.78
$[Fe_2O_2(mhxta)_2(OH)_2]^{4-}$	151	152	425	−7	795		1.79	1.79
$[Fe_2O(N5)Br_2]^+$	151		422		846[d]		1.73	1.80
$[Fe_2O(N5)Cl_2]^+$	150		425		850[d]	−44	1.75	1.78
Dibridged Complexes								
$[Fe_2O(hdp)_2(OBz)]^+$	129	124	494	−17	763	−43	1.78	1.80
$[Fe_2O(hdp)_2(O_2PR_2)]^+$		148	461	−9				
$[Fe_2O(tpa)_2(OBz)]^{2+}$	130	124	497	−17	772[d]	−37	1.77	1.81
$[Fe_2O(tpa)_2(OAc)]^{2+}$	129		499		770[d]	−38	1.78	1.79
$[Fe_2O(tpa)_2(O_2PR_2)]^{2+}$	158		454		778		1.78	1.82
Tribridged Complexes								
$[Fe_3O(tacn)_2(OAc)_3]^{2+}$	119	130	540	−17	749	−33	1.78	1.78
$[Fe_3O(mtacn)_2(OAc)_3]^{2+}$	120		537				1.80	1.80
$[Fe_3O(N3)_2(OBz)_2]^{2+}$	119		537		745	−45	1.78	1.80
$[Fe_3O(tpbn)(OAc)_2]_2^{4+}$	121		525		727[d]		1.79	1.79
$[Fe_3O(tpin)(OAc)_2]_2^{4+}$			540		725			
$[Fe_3O(HBpz)_2)_2(OAc)_2]$	124	128	528	−17	751	−30	1.78	1.79
$[Fe_3O(tmip)_2(OPr)_2]^{2+}$	*e*	129	533	−17[f]	749[d]	−34	*e*	*e*
Proteins								
oxyhemerythrin (HO_2^-)		134	486	−14	753	−37		
methemerythrin (N_3^-)	135	136	507	−14	768	−35	1.64	1.89
methemerythrin (SCN^-)		130	514	−16	780	−38		
methemerythrin (CN^-)		137	512	−14	782	−28		
methemerythrin (OCN^-)		143	509	−12	782	−26		
ribonucleotide reductase	130	138	493	−13	756	−25	1.78	1.78

[a] Observed Fe–O–Fe angles and Fe–O distances (in Å) from X-ray crystal structures of model compounds (references listed in Experimental Procedures) and hemerythrin (ref 5), and from EXAFS of ribonucleotide reductase (ref 32). Calculated Fe–O–Fe angles based on secular equation (ref 33) for ν_s(Fe–O–Fe) with ^{16}O and ^{18}O. [b] Frequencies in cm^{-1}. ν_s from Raman spectroscopy, ν_{as} from IR spectroscopy (model compounds), and Raman spectroscopy (proteins). Values from following sources: Cl-pdc complex ν_{as} (ref 13), TPP complex (ref 34a), hedta complex ν_{as} (ref 25a), Cl_6 complex (ref 34b), phen complex (ref 10), mhxta complex (ref 19), N5 complex (ref 14b), hdp and tpa complexes (ref 20b), tacn complex (ref 35), N3 complex ν_{as} (ref 36), tpin complex ν_{as} (ref 18), $HBpz_3$ complex (ref 37), hemerythrin complexes (ref 22), ribonucleotide reductase (ref 7b). All other values from this work. [c] Isotope shift determined for ν_s(Fe–O–Fe) at 423 cm^{-1} in aqueous solution at 15 K. [d] ν_{as} obtained from Raman spectrum. [e] Isostructural $[Fe_2O(tmip)_2(OAc)_2](ClO_4)_2$ complex has Fe–O–Fe angle of 123° and Fe–O distance of 1.80 Å (ref 14d). [f] Determined from $2\nu_s$ due to Fermi resonance of ν_s in ^{18}O sample.

1.3 Vibrational Spectroscopy

Table I. Vibrational Frequencies and Parameters of Oxo-Bridged Fe(III) Complexes

sample	Fe–O–Fe angle[a]		Fe–O–Fe stretch[b]				Fe–O distances[a]	
	obs	calc	ν_s	$\Delta^{18}O$	ν_{as}	$\Delta^{18}O$	Fe 1	Fe 2
			Monobridged Complexes					
$[Fe_2O(Cl\text{-}pdc)_2(H_2O)_4]$	180		381		850		1.77	1.77
$[Fe_2O(TPP)]$	175		363		885		1.76	1.76
$[Fe_2O(hedta)_2]^{2-}$	165	167	409	−2[c]	838		1.80	1.79
$[Fe_2O(n\text{-propsal})_4]$	164		403		860		1.76	1.78
$[Fe_2OCl_6]^{2-}$	156		458	−18	870	−44	1.76	1.76
$[Fe_2O(phen)_4(H_2O)_2]^{4+}$	155	156	395	−5	827	−39	1.78	1.78
$[Fe_4O_2(mhxta)_2(OH)_2]^{4-}$	151	152	425	−7	795		1.79	1.79
$[Fe_2O(N5)Br_5]^{+}$	151		422		846[d]		1.73	1.80
$[Fe_2O(N5)Cl_3]^{+}$	150		425		850[d]	−44	1.75	1.78
			Dibridged Complexes					
$[Fe_2O(hdp)_2(OBz)]^{+}$	129	124	494	−17	763	−43	1.78	1.80
$[Fe_2O(hdp)_2(O_2PR_2)]^{+}$		148	461	−9				
$[Fe_2O(tpa)_2(OBz)]^{3+}$	130	124	497	−17	772[d]	−37	1.77	1.81
$[Fe_2O(tpa)_2(OAc)]^{3+}$	129		499		770[d]	−38	1.78	1.79
$[Fe_2O(tpa)_2(O_2PR_2)]^{3+}$	138		454		778		1.78	1.82
			Tribridged Complexes					
$[Fe_2O(tacn)_2(OAc)_2]^{2+}$	119	130	540	−17	749	−33	1.78	1.78
$[Fe_2O(mtacn)_2(OAc)_2]^{2+}$	120		537				1.80	1.80
$[Fe_2O(N3)_2(OBz)_2]^{2+}$	119		537		745	−45	1.78	1.80
$[Fe_2O(tpbn)(OAc)_2]_2^{4+}$	121		525		727[d]		1.79	1.79
$[Fe_2O(tptn)(OAc)_2]_2^{4+}$			540		725			
$[Fe_2O(HBpz_3)_2(OAc)_2]$	124	128	528	−17	751	−30	1.78	1.79
$[Fe_2O(tmip)_2(OPr)_2]^{2+}$	*e*	129	533	−17[f]	749[d]	−34	*e*	*e*
			Proteins					
oxyhemerythrin (HO_2^-)		134	486	−14	753	−37		
methemerythrin (N_3^-)	135	136	507	−14	768	−35	1.64	1.89
methemerythrin (SCN^-)		130	514	−16	780	−38		
methemerythrin (CN^-)		137	512	−14	782	−28		
methemerythrin (OCN^-)		143	509	−12	782	−26		
ribonucleotide reductase	130	138	493	−13	756	−25	1.78	1.78

[a] Observed Fe–O–Fe angles and Fe–O distances (in Å) from X-ray crystal structures of model compounds (references listed in Experimental Procedures) and hemerythrin (ref 5), and from EXAFS of ribonucleotide reductase (ref 32). Calculated Fe–O–Fe angles based on secular equation (ref 33) for ν_s(Fe–O–Fe) with ^{16}O and ^{18}O. [b] Frequencies in cm^{-1}. ν_s from Raman spectroscopy, ν_{as} from IR spectroscopy (model compounds), and Raman spectroscopy (proteins). Values from following sources: Cl–pdc complex ν_{as} (ref 13), TPP complex (ref 34a), hedta complex ν_{as} (ref 25a), Cl_6 complex (ref 34b), phen complex (ref 10), mhxta complex (ref 19), N5 complex (ref 14b), hdp and tpa complexes (ref 20b), tacn complex (ref 35), N3 complex ν_{as} (ref 36), tptn complex ν_{as} (ref 18), $HBpz_3$ complex (ref 37), hemerythrin complexes (ref 22), ribonucleotide reductase (ref 7b). All other values from this work. [c] Isotope shift determined for ν_s(Fe–O–Fe) at 423 cm^{-1} in aqueous solution at 15 K. [d] ν_{as} obtained from Raman spectrum. [e] Isostructural $[Fe_2O(tmip)_2(OAc)_2](ClO_4)_2$ complex has Fe–O–Fe angle of 123° and Fe–O distance of 1.80 Å (ref 14d). [f] Determined from $2\nu_s$ due to Fermi resonance of ν_s in ^{18}O sample.

Course Outline

1. Symmetry, Group Theory, and Electronic Structure

1.1 Fundamentals

1.2 Symmetry and Group Theory

1.3 Vibrational Spectroscopy

2. Ground State Spectroscopic Methods

3. Excited State Spectroscopic Methods

4. Other Physical Methods